



# Multifactorial analysis of terminator performance on heterologous gene expression in *Physcomitrella*

Paul Alexander Niederau<sup>1</sup> · Pauline Eglé<sup>1</sup> · Sandro Willig<sup>1</sup> · Juliana Parsons<sup>1</sup> · Sebastian N. W. Hoernstein<sup>1</sup> · Eva L. Decker<sup>1</sup> · Ralf Reski<sup>1,2</sup>

Received: 13 July 2023 / Accepted: 2 November 2023 / Published online: 22 January 2024  
© The Author(s) 2024

## Abstract

**Key message** Characterization of *Physcomitrella* 3'UTRs across different promoters yields endogenous single and double terminators for usage in molecular pharming.

**Abstract** The production of recombinant proteins for health applications accounts for a large share of the biopharmaceutical market. While many drugs are produced in microbial and mammalian systems, plants gain more attention as expression hosts to produce eukaryotic proteins. In particular, the good manufacturing practice (GMP)-compliant moss *Physcomitrella* (*Physcomitrium patens*) has outstanding features, such as excellent genetic amenability, reproducible bioreactor cultivation, and humanized protein glycosylation patterns. In this study, we selected and characterized novel terminators for their effects on heterologous gene expression. The *Physcomitrella* genome contains 53,346 unique 3'UTRs (untranslated regions) of which 7964 transcripts contain at least one intron. Over 91% of 3'UTRs exhibit more than one polyadenylation site, indicating the prevalence of alternative polyadenylation in *Physcomitrella*. Out of all 3'UTRs, 14 terminator candidates were selected and characterized via transient Dual-Luciferase assays, yielding a collection of endogenous terminators performing equally high as established heterologous terminators CaMV35S, AtHSP90, and NOS. High performing candidates were selected for testing as double terminators which impact reporter levels, dependent on terminator identity and positioning. Testing of 3'UTRs among the different promoters NOS, CaMV35S, and PpActin5 showed an increase of more than 1000-fold between promoters PpActin5 and NOS, whereas terminators increased reporter levels by less than tenfold, demonstrating the stronger effect promoters play as compared to terminators. Among selected terminator attributes, the number of polyadenylation sites as well as polyadenylation signals were found to influence terminator performance the most. Our results improve the biotechnology platform *Physcomitrella* and further our understanding of how terminators influence gene expression in plants in general.

**Keywords** Molecular pharming · Moss · Plant biotechnology · UTR · *Physcomitrium*

## Introduction

The biotechnology sector is estimated to have an economic potential of around 3 trillion USD per year in 2030–2040, not considering downstream and secondary effects (Chui et al. 2020). A large share is attributed to the biopharmaceutical

market and the production of recombinant proteins for health applications. While the most established production platforms are based on bacteria, yeast, insect, and mammalian cells; plants are an attractive alternative for producing eukaryotic proteins (Reski et al. 2015; Rybicki 2020; He et al. 2021; Lobato Gómez et al. 2021).

Plant-based expression systems can operate at lower cost, possess high scalability, produce complex and highly glycosylated proteins, and are free of human pathogens and endotoxins (Twyman et al. 2003; Lomonosoff and D'Aoust 2016; Capell et al. 2020). The most used plant in molecular pharming is *Nicotiana benthamiana*, which has been successfully glyco-engineered to produce ZMapp, a treatment for Ebola based on an antibody cocktail lacking plant-typical *N*-glycan modifications (Margolin et al. 2018). Other

Communicated by Peishan Yi.

✉ Ralf Reski  
ralf.reski@biologie.uni-freiburg.de

<sup>1</sup> Plant Biotechnology, Faculty of Biology, University of Freiburg, Freiburg, Germany

<sup>2</sup> Signalling Research Centre BIOS and CIBSS, University of Freiburg, Freiburg, Germany

promising plant-produced pharmaceuticals still in clinical trials are virus-like particles (VLPs)-based vaccines such as the hemagglutinin-based influenza VLP (D'Aoust et al. 2010; Ward et al. 2020). A promising alternative plant for producing biopharmaceuticals is the GMP (good manufacturing practice)-compliant moss *Physcomitrella* (*Physcomitrium patens*) (Reski et al. 2018; Decker and Reski 2020). *Physcomitrella* has an excellent genetic amenability due to its haploid dominant phase and its high rate of homologous recombination enabling precise gene targeting (Strepp et al. 1998; Reski 2018). Plant-specific  $\beta$ 1,2-xylosylation,  $\alpha$ 1,3-fucosylation,  $\beta$ 1,3-galactosylation, and formation of Lewis A epitopes on *N*-glycans could be abolished via targeted gene knockouts yielding more humanized and homogenic *N*-glycan patterns (Koprivova et al. 2004; Parsons et al. 2012). Another recent advance was the introduction of enzymes necessary for sialic acid synthesis, activation, and linkage to protein *N*-glycans (Bohlender et al. 2020). The protein  $\alpha$ -galactosidase A (aGal) produced in *Physcomitrella* bioreactors (<https://www.elevabiologics.com/>), intended to treat Morbus Fabry, successfully passed clinical phase I (Shen et al. 2016; Hennermann et al. 2019). Other moss-based products in the pre-clinical phase are human factor H (FH) and synthetic FH-related multitarget proteins MFHR1 and MFHR13. These glycoproteins act as regulators of the human complement system and are potential biopharmaceuticals for treatment of complement-related disorders (Büttner-Mainik et al. 2011; Michelfelder et al. 2017, 2018; Top et al. 2019; Ruiz-Molina et al. 2022a).

A critical factor for choosing a biotechnology production platform for a drug candidate is product yield. To increase yields, bioprocess design is used at different steps during the production workflow. Upstream processes typically deal with genetic engineering of cell lines, bioreactor growth kinetics, media compositions, etc., whereas downstream processes focus on harvest, purification, and formulation of the final product. In *Physcomitrella*, various efforts were made to optimize media compositions (Schween et al. 2003) and the kinetic models of biomass growth and recombinant protein production under the impact of phytohormone addition and bioreactor operation modes were described recently (Ruiz-Molina et al. 2022b). Further efforts have been made to select and characterize elements of gene expression regulation for the design of expression constructs encoding recombinant proteins. Various endogenous and heterologous promoter sequences were evaluated (Horstmann et al. 2004; Jost et al. 2005; Gitzinger et al. 2009), including the *Physcomitrella*-derived Actin5 promoter as the highest yielding promoter for molecular pharming purposes (Weise et al. 2006). In addition, secretion signals have been characterized for their effects on protein yield and secretion efficiency which facilitate downstream purification of protein products (Schaaf et al. 2005; Gitzinger et al. 2009). Finally, codon

optimization of heterologous cDNAs successfully increased recombinant protein yields by preventing unwanted hetero-splicing, which causes truncated target protein forms (Top et al. 2021). Another crucial element of gene expression with the potential to increase product yields are terminators. However, engineering and investigating terminators to enhance heterologous gene expression are still a neglected area compared to other yield optimization strategies.

Terminators are crucial for high recombinant protein yields by acting on transcription, pre-mRNA processing, mRNA stability, and translation (Moore and Proudfoot 2009; Zhong et al. 2023; Liu et al. 2023). At the start of transcription, the gene promoter and terminator interact in a process called gene looping. This interaction is mediated via transcription factors bound to the gene's 5' end and components of the polyadenylation (polyA) complex bound to the conserved polyA signal (PAS) 5'-AATAAA-3' at the gene's 3' end (Tan-Wong et al. 2009, 2012). Gene loops facilitate RNA Polymerase II (pol II) recycling, transcriptional directionality and play a role in transcriptional memory by interacting with nuclear pores, thereby facilitating transcriptional re-induction and transcript transport (Tan-Wong et al. 2009, 2012). The immature transcript is subsequently processed in a two-step reaction. First, the pre-mRNA is cleaved 10–30 bases downstream of the PAS (Bentley 2005; Mandel et al. 2008). Subsequently, a polyA polymerase (PAP) adds 50–200 adenine residues to the polyA site, marking the end of transcription. The presence of the polyA tail is a prerequisite for the interaction with the polyA-binding protein (PABP) and determines the downstream fate of the mRNA. Most transcripts undergo alternative polyadenylation (APA), a process in which a pre-mRNA is processed into multiple mRNAs that differ in their 3'UTR lengths (Guo et al. 2016; Mayr 2016). The RNA–protein complex mediates the export into the cytoplasm and slows down mRNA degradation by 3' exonucleases, thereby promoting mRNA stability which is linked to higher protein levels (Mandel et al. 2008). Improperly polyadenylated transcripts, in turn, are degraded faster. The polyA-bound PABP interacts with translation initiation factors present at the 5' cap of the mRNA resulting in the formation of mRNA loops which facilitate ribosomal recycling and increase translation efficiency (Hoshino 2012; Paek et al. 2015; Choe et al. 2018). Ultimately, ongoing de-adenylation of the polyA tail leads to PABP uncoupling and activation of the mRNA decay pathway. Hence, proper 3' end processing of transcripts is essential to ensure efficient translation.

Although members of the polyA complex and other protein factors involved in pre-mRNA 3' processing are somewhat conserved between mammals, yeast, and plants, the RNA motifs involved differ between them (Zhao et al. 2009). In plants, polyadenylation is mediated via four main motifs, namely the cleavage element (CE) containing the cleavage

site (CS) or polyA site, the near upstream element (NUE), and the far upstream element (FUE) (Rothnie 1996; Li & Hunt 1997; Rothnie et al. 2001; Loke et al. 2005). The CS consists of the dinucleotide motif YA (CA or UA) and is located at position -1 and -2 of the point of cleavage. The CE motif is U-rich and comprises 10 bases up- and downstream from the CS. The FUE spans 6–18 bases, is located 50 bases upstream of the CS, and acts as an enhancer element which is less defined in its nucleotide composition but rich in U and G. The NUE locates 13–30 bases upstream of the CS and comprises the PAS (5'-AATAAA-3'). While highly conserved in mammals, in plants, the NUE can span between 5 and 10 bases and is more diverse. In the angiosperm *Arabidopsis thaliana*, 5'-AATAAA-3' is the major NUE but comprises only 10% of all identified motifs, whereas TGTA is the major NUE motif in the alga *Chlamydomonas reinhardtii* (Loke et al. 2005; Wodniok et al. 2007).

Despite the important role of terminators in modulating gene expression, little attention has been paid to enhancing recombinant protein yields by analysing and engineering terminator sequences in plants. This is emphasized by the fact that the nopaline synthase (NOS) terminator from *Agrobacterium tumefaciens* and the cauliflower mosaic virus CaMV 35S terminator have been used in plant-based expression systems for decades (Pietrzak et al. 1986; Macfarlane et al. 1992). An improvement of this terminator setup was the application of the *Arabidopsis* heat shock protein (HSP) 90 terminator. This terminator increased the expression of a GUS reporter gene twofold compared to the NOS terminator in transiently as well as in stably transformed plants (Nagaya et al. 2010). Terminators moved further into the spotlight resulting in a range of new insights affecting plant biotechnology. In *N. benthamiana*, an intronless version of the *N. tabacum* extensin (EU) terminator was characterized and achieved a threefold increase in signal strength compared to its intron-containing version and a 13.6-fold increase compared to the NOS terminator (Diamos and Mason 2018; Rosenthal et al. 2018). Combining NtEUt in chimeric double terminators with NOST, 35St, and AtHSP90t further increased reporter levels up to 37.7-fold. Here, synergistic effects were observed between terminator pairs depending on their identity, positioning (1st or 2nd), and heterogeneity (heterologous pairs outperformed homologous pairs). This led to the suggestion that double terminators exhibit a more stringent transcription termination signal resulting in less read-through transcripts and less RDR6-mediated silencing of the transcript (Luo and Chen 2007; Beyene et al. 2011; Diamos and Mason 2018). High reporter levels caused by heterologous double terminators could also be linked to enhanced interactions of the terminators with the 5'UTR and the associated machinery (Andreou et al. 2021). By characterizing 15 terminators across a range of five different

promoters, Andreou et al. (2021) found synergistic interactions between promoters and terminators. However, equivalent data from non-flowering plants like mosses are lacking.

In this study, we analysed 3'UTRs from *Physcomitrella* and selected and characterized putative terminator candidates. We identified endogenous terminators performing equally high as the commonly employed terminator CaMV35S. We then fused high performing candidates in different combinations as double terminators and tested their performance in combination with three promoters PpActin5, CaMV35S, and NOS to further develop the biopharmaceutical production platform *Physcomitrella*.

## Materials and methods

### Plant material

*Physcomitrella* wild type (new species name: *Physcomitrium patens* (Hedw.) Mitt.; (Medina et al. 2019)), ecotype “Gransden 2004” (IMSC acc. No. 40001), was cultivated axenically in mineral KnopME medium 250 mg/L  $\text{KH}_2\text{PO}_4$ , 250 mg/L KCl, 250 mg/L  $\text{MgSO}_4$ , 1 g/L  $\text{Ca}(\text{NO}_3)_2$ , 12.5 mg/L  $\text{FeSO}_4$ , including microelements (50  $\mu\text{M}$   $\text{H}_3\text{BO}_3$ , 50  $\mu\text{M}$   $\text{MnSO}_4 \times \text{H}_2\text{O}$ , 15  $\mu\text{M}$   $\text{ZnSO}_4 \times 7 \text{H}_2\text{O}$ , 2.5  $\mu\text{M}$  KJ, 0.5  $\mu\text{M}$   $\text{Na}_2\text{MoO}_4 \times 2 \text{H}_2\text{O}$ , 0.05  $\mu\text{M}$   $\text{CuSO}_4 \times 5 \text{H}_2\text{O}$ , 0.05  $\mu\text{M}$   $\text{CoCl}_2 \times 6 \text{H}_2\text{O}$ ) (Reski and Abel 1985; Egner et al. 2002; Schween et al. 2003; Decker et al. 2015). The pH was adjusted to 5.8 with KOH and media were sterilized by autoclaving. The standard growth conditions were 22 °C with a 16-h/8-h light/dark photoperiod and light intensity of 50–70  $\mu\text{mol}/\text{m}^2/\text{s}^1$ . Flasks were incubated on rotating shakers with 125 rpm speed. Plant material was disrupted using an ULTRA-TURRAX (IKA, Staufen im Breisgau, Germany) at 18,000 rpm for 60 s and transferred to fresh KnopME media every 7 days.

### Characterization of 3'UTRs for length, presence of introns, and poly(A) sites

A fasta file containing the latest *Physcomitrella* genome assembly (V3.3, Lang et al. 2018) was downloaded from the Phytozome database (<https://phytozome-next.jgi.doe.gov/>, Goodstein et al. 2012) and the annotated UTR sequences of 75,790 transcripts were extracted based on coordinates available from the corresponding gff3 file using a custom Perl script, also available from Phytozome. Redundant UTR sequences were removed using the “delete duplicates” Excel-function. The length of each sequence was calculated using the Excel-function “LEN”. The “COUNTIF” function was used to count the number of 3'UTRs having an intron (“int”) and not having an intron (“no\_int”). To predict the number of poly(A) sites in each 3'UTR, the Poly(A) Site

Sleuth (PASS) tool for poly(A) site prediction in plants (Ji et al. 2007, 2015) was used. For that purpose, all sequences smaller than 50 were removed yielding 52,952 sequences. The PASS2.0 software package for poly(A) site prediction was performed at default configurations.

### Selection of terminator candidates

The first selection of terminator candidates was based on microarray data from Hoernstein et al. (2018) (<https://www.ebi.ac.uk/arrayexpress/experiments/E-MTAB-5374/files/>) which included the expression levels of the transcripts of the Doko#69 line (Eleva GmbH, Freiburg, Germany, IMSC Acc. No. 40828). The translation of gene names from the V1.6 annotation to the newest V3.3 gene model (Lang et al. 2018) was performed with the aid of the Phytozome database (Goodstein et al. 2012). The sequence of the 3'UTR for each gene, the presence of introns, the strand, and the coordinates of the 3'UTR were imported from the corresponding gff3 file, also available at Phytozome (<https://phytozome-next.jgi.doe.gov/>, Goodstein et al. 2012). All genes without an annotated 3'UTR were excluded from the list. For each gene containing an intron in the 3'UTR, their sequence was analysed manually on Phytozome to determine the length of the exons. Redundant UTR sequences were removed using the “delete duplicates” Excel-function. miRNA-binding sites were analysed using the tool psRNAtarget (Dai & Zhao 2011; Dai et al. 2018) containing 280 published miRNAs sequences using the pre-selected parameters (scoring scheme V2 (2017), accessed on 12th of May 2020). The Gene Ontology (GO) search was performed based on GO annotation downloaded from the PEATmoss database ([https://peatmoss.plantcode.cup.uni-freiburg.de/downloads/Annotations/P.patens\\_lookup\\_table\\_20181029.xlsx](https://peatmoss.plantcode.cup.uni-freiburg.de/downloads/Annotations/P.patens_lookup_table_20181029.xlsx), Perroud et al. (2018), Fernandez-Pozo et al. (2020)).

### Construction of plasmids

The normalization vector 35Sp-Rluc-35St comprising the *Renilla* luciferase originates from Horstmann et al. (2004) (Supplementary File S1.1). The expression cassette consists of a long version of the CaMV 35S promoter, the *Renilla* luciferase coding sequence (CDS), and the CaMV 35S terminator. The testing vectors comprising the firefly luciferase were adapted from the 35Sp-Fluc-35St initially described by Horstmann et al. (2004) (Supplementary File S1.2). Single terminator testing vectors were obtained by restriction-ligation cloning using restriction enzymes PstI and BglIII. In that case, 35Sp-Fluc-35St was used as a template from which the 35S terminator was removed via digestion using PstI and BglIII. New terminator candidates were amplified using Phusion Polymerase (Thermo Fisher Scientific Inc., Waltham, USA). PstI and BglIII restriction enzyme sites were

added to the template via overhang extension PCR for subsequent ligation into the firefly template vector. Alternatively, a Golden Gate-like one-pot cloning reaction using type IIS enzymes Eco31I and Esp3I was used. For that purpose, the template Pro-Fluc-Ter\_GG placeholder vector (Supplementary File S1.3) was obtained by removing Eco31I and Esp3I restriction sites in the template vector 35Sp-Fluc-35St. One Eco31I in the ampicillin selection marker was removed by site-directed mutagenesis via PCR. Two Esp3I restriction enzyme recognition sites were removed by deleting a 51 bp large segment in the non-coding backbone. The 35S promoter and terminator were removed and substituted by a 32 and 33 bp spanning placeholder element bearing outwards facing recognition sites for the type IIS enzymes Esp3I and Eco31I, respectively. The placeholder vector Pro-Fluc-Ter\_GG and PCR amplicons for the promoter and terminator region containing Esp3I and Eco31I recognition sites, respectively, were fused with T4 Ligase, 0.5 mM ATP and the restriction enzymes in 1×Fast Digest buffer (Thermo Fisher Scientific Inc., Waltham, USA). The reaction mixture was incubated for 1 min at 37 °C and 1 min at 16 °C for in total 30 cycles. Ligated vectors were transformed into *E. coli* DH5α and positive clones were selected via Colony PCR using Taq polymerase (VWR, Radnor, USA). Correct insertion was checked via Sanger sequencing at Eurofins Genomics (Ebersberg, Germany). Primers were synthesized by Eurofins Genomics and are listed in Supplementary table S2. All vectors used in this study are listed in Supplementary table S3.

### Protoplast preparation

For protoplast preparation, existing protocols (Hohe and Reski 2002) were adapted. Here, 100–200 mL protonema suspension from flasks cultivated in KnopME medium pH 4.5 were used as starting material (around 250 mg/L of dry weight). Plant material was disrupted as described above 7 days prior to protoplast preparation. In addition, 1 day prior to isolation of protoplasts the plant material was transferred to fresh media at pH 4.5. Moss material was incubated in the dark for 2 h in 0.5 M mannitol (adjusted to pH 5.8 with KOH, adjusted to 560 mOs using mannitol, sterilized by autoclaving) containing 1% Driselase (w/v). Subsequently, the moss material was passed through a 100 μm and a 50 μm sieve to separate protonema filaments from protoplasts. Recovered protoplasts were washed twice using 0.5 M mannitol solution before determining the protoplast number using a Fuchs-Rosenthal-counting chamber. Protoplasts were centrifuged and resuspended in 3 M media (0.5 M mannitol, 15 mM MgCl<sub>2</sub>, 0.1% MES, pH adjusted to 5.6 with KOH, and osmolarity adjusted to 580 mOs using mannitol) resulting in a density of  $1.2 \times 10^6$  protoplasts/mL.

## Protoplast transformation

For moss protoplast transformation, existing protocols (Hohe and Reski 2002; Hohe et al. 2004; Decker et al. 2015) were adapted for usage in a 96-well format. Both firefly and *Renilla* vectors were applied in equimolar concentrations across samples within one experiment. To ensure readout values were within the linear spectrum, the ratios of firefly to *Renilla* luciferase vectors were adjusted for different experiments. For each transformation, 63  $\mu\text{L}$  of protoplast suspension was mixed with 25  $\mu\text{L}$  of DNA in 0.1 M  $\text{Ca}(\text{NO}_3)_2$  and 88  $\mu\text{L}$  of 40% (w/w) PEG solution in a round-bottom 1 mL 96 deep-well plate (Nunc®, Roskilde, Denmark). The PEG solution was prepared by mixing 8 g of PEG (polyethylene glycol, MW4000) with 12 g of 3 M media. The transformation mixture was incubated in a 96-well plate for 30 min on a rotary shaker at medium intensity. Protoplasts were washed twice with 500  $\mu\text{L}$  3 M media, gently mixed, centrifuged for 10 min at 50 $\times g$  with slow acceleration and slow deceleration. The supernatant was discarded. Collected protoplasts were resuspended in 500  $\mu\text{L}$  regeneration medium (KnopME + 50 g/L glucose and 30 g/L mannitol). Transfected protoplasts were incubated at 22 °C for 24 h in the dark and subsequently for 24 h at a 16-h/8-h light/dark photoperiod and light intensity of 50–70  $\mu\text{mol}/\text{m}^2/\text{s}^1$ .

## Dual-Luciferase assays

Luciferase levels were detected using the Dual-Luciferase® Reporter Assay System (Promega, Madison, USA). Cells were centrifuged at 850 $\times g$  for 10 min and the supernatant was discarded. Protoplasts were resuspended in 80  $\mu\text{L}$  passive lysis buffer (Promega) on a rotary shaker for 30 min at 4 °C. To remove cell debris, samples were centrifuged for 1 min at 4 °C at 2250 $\times g$ . For each transformation, 3  $\times$  20  $\mu\text{L}$  of supernatant were transferred to a white flat-bottom 96-well-microplate (Greiner, Kremsmünster, Austria) to obtain three technical replicates. In the same sample, firefly luminescence was detected by adding 100  $\mu\text{L}$  LARII reagent (Promega) and *Renilla* luciferase activity was detected by adding 100  $\mu\text{L}$  Stop&Glo (Promega) reagent. Detection was performed in a POLARstar Omega microplate reader (BMG Labtech, Ortenberg, Germany) with shaking of the plate and a 1 s settling time after reagent injection and a 10 s read time. Normalized expression is reported as the ratio of luminescence from the firefly test construct to the *Renilla* calibrator. For each terminator candidate, at least three independent transformations were performed and evaluated ( $n \geq 3$  biological replicates). For each biological replicate, the mean of three technical replicates was recorded and the resulting values were normalized to 35Sp35St.

## Statistical analysis

The firefly-luc/*Renilla*-luc reporter values of terminator candidates obtained were normalized to the control 35Sp35St before analysis via one-way ANOVA and Tukey HSD test using RStudio (version: 2022.07.2). Pearson correlation coefficients were calculated in Microsoft Excel 2019 between reporter values and the respective criteria, such as number of polyA sites, number of polyA signals, expression values, and 3'UTR length (bp). The principal component analysis (PCA) and subsequent clustering using the package 'Mclust' (Fraley and Raftery 2003) were generated using RStudio (version: 2022.07.2).

## Results

### Prevalence of alternative polyadenylation

For the *Physcomitrella* genome, 87,533 transcripts are annotated of which 75,753 have an annotated 3'UTR (Supplementary Table S4.1; Lang et al. 2018). Due to alternative splicing, several transcripts encoded from the same genomic locus can have the same 3'UTR. Here, only unique UTR sequences were kept for further analysis, resulting in 53,346 3'UTR sequences (Supplementary Table S4.2). Of those unique sequences, 7964 have at least one intron and 45,382 do not have an intron (Fig. 1). The average length of 3'UTRs is 654 bp and the median length is 524 bp (Fig. 1A). For 3'UTRs without intron, the average and the median length is 542 bp and 471 bp respectively, whereas 3'UTRs with introns are more than twice as long with an average of 1293 bp and a median of 1114 bp (Fig. 1B, C).

The list was further reduced by removal of all transcripts smaller than 50 bp to allow for poly(A) site prediction. The resulting 52,947 transcripts were analysed using the PASS 2.0 software (Ji et al. 2007, 2015) to identify the location and number of poly(A) sites of each 3'UTR. Whereas around 3,607 and 1,025 transcripts exhibit no or one poly(A) site, respectively, the vast majority of 3'UTRs contain multiple poly(A) sites. In fact, > 91% of transcripts were predicted to have two or more poly(A) sites (Fig. 1D).

### Selection of 3'UTRs yields 14 terminator candidates

To identify endogenous terminators yielding high expression in *Physcomitrella*, to be used in molecular pharming, two different approaches were followed as depicted in Fig. 2. For the first approach based on transcript abundance, a list of 3'UTR candidates was generated based on microarray data generated by Hoernstein et al. (2018) (Supplementary Table S5.1). Here, the microarray data from the *Physcomitrella* Doko#69 line were utilized, since this line is

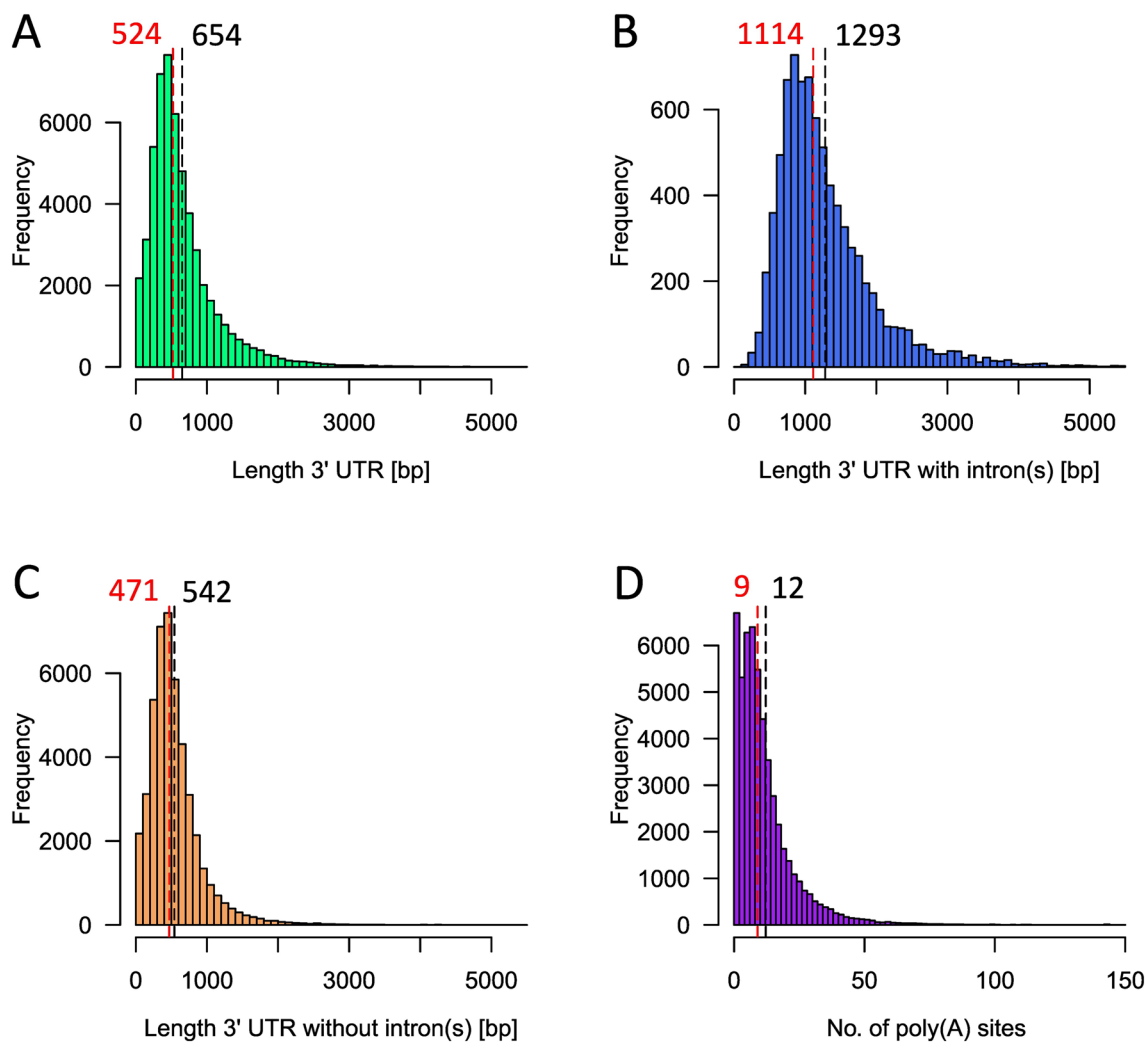


**Fig. 1** Analysis of 3'UTRs in *Physcomitrella*. **A** Length distribution of all 53,346 unique 3'UTRs. **B** Length distribution of unique 3'UTRs with intron(s). **C** Length distribution of unique 3'UTRs without intron(s). In **A**, **B**, & **C** sequences longer than 5500 bp were excluded. **D** Number of poly(A) sites predicted via PASS 2.0 software (Ji et al.

2007, 2015). For poly(A) site prediction, only sequences longer than 50 bp were applicable, reducing the dataset to 52,947 sequences. The red and black dashed lines and numbers indicate the median and average, respectively

the platform line used by Eleva (Eleva GmbH, Freiburg, Germany) for producing biopharmaceuticals. The Doko#69 line is a double knockout for genes encoding an  $\alpha$ 1,3-fucosyltransferase and a  $\beta$ 1,2-xylosyltransferase, which are responsible for the addition of potentially allergenic sugar residues to proteins (Koprivova et al. 2004). Consequently, genes highly expressed in this line are considered to be highly expressed under bioproduction conditions. The 3'UTRs of the transcripts were ranked according to the highest expression average of their corresponding transcript and the top 200 were kept for further analysis. The microarray data were based on genome version 1.6 (Zimmer et al. 2013), and hence, gene IDs of the top 200 candidates were converted into version 3.3 accessions to enable further comparisons. In this step the list of candidates increased from

200 to 263, since several genes annotated in the V1.6 version had multiple matches in the V3.3 version and therefore multiple sequences (Supplementary Table S5.2). After deletion of redundant sequences corresponding to splice variants within the annotation V3.3, and those without known 3'UTR sequences, 223 genes remained (Supplementary Table S5.3). Long 3'UTRs are linked to mRNA decay pathway activation and shorter mRNA half-lives in *Arabidopsis*, *N. benthamiana*, and yeast (Kertész et al. 2006; Yamanishi et al. 2013; Srivastava et al. 2018). Further, the goal was to obtain terminator candidates of short length to facilitate expression construct assembly and genome integration for future molecular pharming applications. With respect to the determined average 3'UTR lengths shown in Fig. 1, a 400 bp cut-off threshold was chosen yielding 65 sequences.

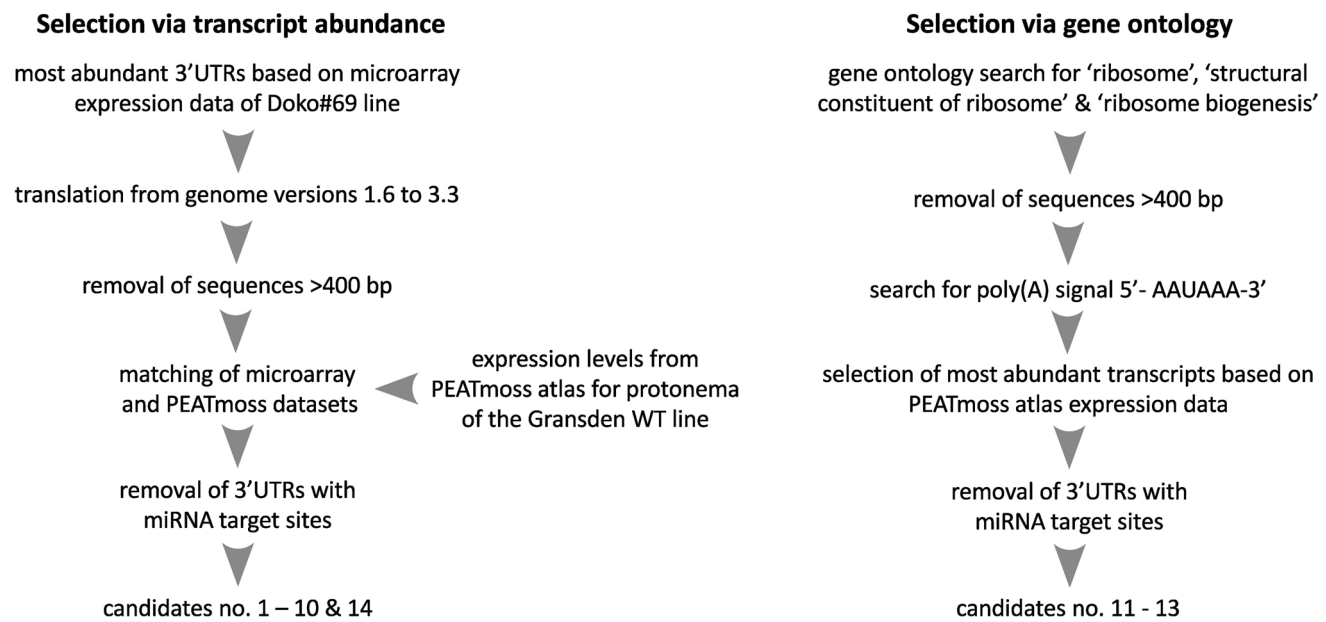


**Fig. 2** Terminator candidate selection workflow. The terminator candidate list was created by selecting transcripts either via abundance or gene ontology and yielded terminators 1–14 as compiled in Table 1

In the case of intron-containing transcripts, the threshold was applied only to the length of the exons, resulting in one intron-containing terminator candidate (UK2, Table 1). Due to difficulties generated by the translation of the gene names, where some sequences of transcripts obtained for the V3.3 annotation corresponded to genes poorly expressed in the original V1.6 annotation of the microarray data, their expression in the Gransden WT line was imported from the PEATmoss expression atlas (Perroud et al. 2018; Fernandez-Pozo et al. 2020). The PEATmoss expression atlas offers expression data for tissues of different developmental stages and growth conditions. Of interest were the expression levels in protonema tissue cultivated in Knop liquid culture (Klq), the tissue and cultivation media used for bioproduction. Comparing the two expression datasets revealed that some genes highly expressed in the Doko#69 (V1.6-based microarray data), were lowly expressed in *Physcomitrella* WT (V3.3-based RNA-seq data, PEATmoss) (Supplementary Table S5.4). Transcripts with no expression values or low values in one of those two datasets were removed from the list, resulting in 39 sequences (Supplementary Table S5.5). Due to APA and other motifs potentially located further downstream of the poly(A) site (Hunt 2008; Li and Du 2014; Srivastava et al. 2018), 100 bp of the downstream genomic sequence were added to the selected 3'UTRs. The list of 44 3'UTRs was checked for possible miRNA-binding sites employing the psRNAtarget tool (Dai et al. 2018). miRNAs are small non-translated RNA molecules which bind complementary sequences in the mRNA and consequently trigger translational inhibition or mRNA degradation

(Jones-Rhoades et al. 2006; Narsai et al. 2007; Khraiwesh et al. 2010). For the set of 43 *Physcomitrella* miRNAs available within psRNAtarget, 52 binding sites were found on 25 different genes (Supplementary Table S5.5). Among the 3'UTRs without a predicted microRNA-binding site, the eight candidates with the highest expression levels in WT were selected (Table 1). An exception was made for a gene encoding a Chlorophyll a/b-binding protein (Cab1, Pp3c13\_7900V3.1). Here, one miRNA-binding site is predicted, but this gene showed the highest expression in that same dataset, yielding nine candidates in total. In addition, UK2 was included as a candidate, since it showed the highest expression values among intron-containing 3'UTRs. However, for molecular characterization, the first exon of 44 bp and the intron of 297 bp were removed. This decision was based on the finding that splicing events in *Physcomitrella* 3'UTRs are positively correlated with nonsense-mediated decay (NMD) of transcripts, a process during which aberrant transcripts are targeted for degradation (Lloyd et al. 2018). Moreover, Rosenthal et al. (2018) showed a threefold increase in signal strength in *N. benthamiana* when removing the intron from the tobacco extensin terminator.

In parallel, a second approach to identify terminator candidates was based on gene ontology (GO). Yamanishi et al. (2013) performed a genome-wide activity assessment in the yeast *Saccharomyces cerevisiae* and found terminators from genes coding for ribosomal proteins yielded high expression of transgenes. Accordingly, a search using the GO terms “ribosome”, “structural constituent of ribosome”, and “ribosome biogenesis” yielded 2109 matches

**Table 1** Final selection of 18 terminator candidates for testing in *Physcomitrella*

#	Gene identifier/source	Gene name	Abbreviation	Expression in protonema Knop suspension culture (FPKM)	Annotation
1	Pp3c13_7900V3.1	chlorophyll a/b-binding protein	Cab1	5428.09	1 × miRNA-binding site, 5 × poly(A) sites, AATAAA motif
2	Pp3c13_6860V3.1	dehydrin	dehyd	2382.07	5 × poly(A) sites
3	Pp3c21_4230V3.1	plastocyanin	petE	1178.96	2 × poly(A) sites
4	Pp3c9_3440V3.1	chlorophyll a/b-binding protein	Cab2	884.36	9 × poly(A) sites
5	Pp3c22_11690V3.1	catalase	Catalase	879.7	1 × poly(A) site
6	Pp3c27_2340V3.1	photosystem II 10 kDa polypeptide	PSII	866.63	2 × poly(A) sites
7	Pp3c12_6700V3.1	Unknown protein	UK	834.25	3 × poly(A) sites
8	Pp3c3_18750V3.1	Ribulose-bisphosphate carboxylase small chain	rbcS	749.16	2 × poly(A) sites
9	Pp3c2_6770V3.1	elongation factor 1-alpha	EF1A	535.83	3 × poly(A) sites
10	Pp3c23_22230V3.1	photosystem I subunit IV	psaE	529.37	6 × poly(A) sites
11	Pp3c3_11250V3.1	60S ribosomal protein L18A	RP-L18A	288.67	5 × poly(A) sites, AATAAA motif
12	Pp3c11_21120V3.1	40S ribosomal protein S6e	RP-S6e	213.83	6 × poly(A) sites, AATAAA motif
13	Pp3c16_2090V3.1	40S ribosomal protein S18e	RP-S18e	213.41	2 × poly(A) sites, AATAAA motif
14	Pp3c16_2460V3.1	Unknown protein 2	(noI)UK2	82.39	10 × poly(A) sites (7 w/o intron), intron, 4 × AATAAA motif (3 w/o intron)
15	GenBank: MN379653.1	35S (Cauliflower Mosaic Virus)	35S	N/A	2 × poly(A) sites, 1 × miRNA-binding site, AATAAA motif
16	Rosenthal et al. (2018)	extensin ( <i>N. tabacum</i> )	EU	N/A	9 × poly(A) sites, 2 × AATAAA motif
17	Andreou et al. (2021)	heat shock protein 90 ( <i>A. thaliana</i> )	HSP90	N/A	8 × poly(A) sites, 2 × miRNA-binding sites, 3 × AATAAA motif
18	Andreou et al. (2021)	nopaline synthase ( <i>Agrobacterium tumefaciens</i> )	NOS	N/A	3 × poly(A) sites, AATAAA motif

Column 2 provides the sequence identifiers of *Physcomitrella* (no. 1–14) or the GenBank identifier or publication for sequences from other organisms (15–18). Columns 3 & 4 list gene names and the abbreviation used in this publication. Column 5 shows the expression (fragments per kilobase of transcript per million mapped reads (FPKM)) values of the candidates for the Gransden WT line cultivated in liquid Knop media (PEATmoss, Fernandez-Pozo et al. 2020). Column 6 contains information about presence of motifs, introns, miRNA-binding sites predicted via psRNATarget using the list of *Physcomitrella* microRNAs and poly(A) sites (predicted in PASS 2.0) (Ji et al. 2007, 2015; Dai et al. 2018). For genes Pp3c12\_6700V3.1 and Pp3c16\_2460V3.1 no putative gene functions are available and therefore named unknown protein and unknown protein 2

in *Physcomitrella* (Supplementary Table S6.1). Many genes matched two or three of the categories. Duplicates were removed, resulting in a list of 1107 unique genes (Supplementary Table S6.2) of which only 3'UTRs with a length between 150 and 401 bp were kept, resulting in 358 genes (Supplementary Tables S6.3 and S6.4). Subsequently, the presence of a 5'-AATAAA-3' signal was checked resulting in 47 3'UTRs (Supplementary Table S6.5). Since the PAS is an important element for mRNA stability and half-life (Rothnie 1996), this step was meant to isolate genes with a higher chance of being correctly processed and subsequently

more stable. After excluding 3'UTR transcripts which were redundant or not expressed in the Gransden WT protonema liquid culture, imported from PEATmoss, 19 genes remained (Supplementary Table S6.6). Using the psRNATarget tool (Dai et al. 2018), the six 3'UTRs with the highest expression were checked for miRNA-binding sites (Supplementary Table S6.7). Finally, three 3'UTRs without miRNA-binding sites were selected as terminator candidates (Table 1).

Finally, the 3'UTR of a Chlorophyll a/b-binding protein (Cab2, Pp3c9\_3440V3.1) was added to the list. This UTR is 511 bp long and therefore exceeds the length threshold of



400 bp introduced earlier. However, Cab2 does not contain predicted miRNA-binding sites, exhibits the fourth highest expression values compared to other selected terminator candidates (Table 1), and contains nine predicted poly(A) sites. To enable comparison of the endogenous terminator candidates the widely used benchmark terminators CaMV35St, NtEUt, AtHSP90t, and NOST were included resulting in a final list of 18 different terminators (Table 1).

### Endogenous terminators yield equally high as the CaMV 35S terminator

To systematically evaluate the 18 individual terminator candidates selected (Table 1), we performed Dual-Luciferase assays. Consequently, we cloned expression constructs containing the firefly luciferase CDS under control of the 35S promoter and the respective terminator candidates. Activity of the transiently expressed reporters was measured 48 h after PEG-mediated transfection of these vectors in *Physcomitrella* protoplasts. To allow for reliable screening of large vector libraries, a 96-well plate-based transformation protocol for *Physcomitrella* protoplasts was established. Differences in transformation efficiency between samples were normalized with the activity of the co-transfected *Renilla* luciferase under control of the 35S promoter and 35S terminator.

From the tested single terminators, eight candidates showed no difference to the reference terminator 35S, including the heterologous terminators AtHSP90, NOS, and NtEU (Fig. 3). In addition, *Physcomitrella*-derived terminators PpRPS6et, PpnoIUK2t, PpCab2t, PpCab1t, and PppetEt performed as well as 35St. However, several endogenous terminators showed a significantly lower performance compared to 35St. Furthermore, there was no significant difference in the performance of the NOS terminator and the NtEU terminator (Fig. 3, NOST, NtEUt). This is in contrast to Rosenthal et al. (2018), who found NtEUt to increase reporter levels by 13.3-fold in *N. benthamiana* as compared to NOST (Diamos and Mason 2018; Rosenthal et al. 2018). The lowest performing terminator is PpUKt at 0.14, 7.9 times lower than the highest performing terminator AtHSP90t. We could identify *Physcomitrella* endogenous terminators performing as well as the widely used 35S terminator. Subsequently, we tested combinations of our best performing terminators in double terminator constructs.

### Endogenous double terminators up to threefold more efficient than respective single terminators

Combining two terminators in tandem in one construct was shown to increase reporter signal levels in various angiosperms, including *Arabidopsis* and *N. benthamiana* (Luo and Chen 2007; Beyene et al. 2011; Yamamoto et al. 2018;

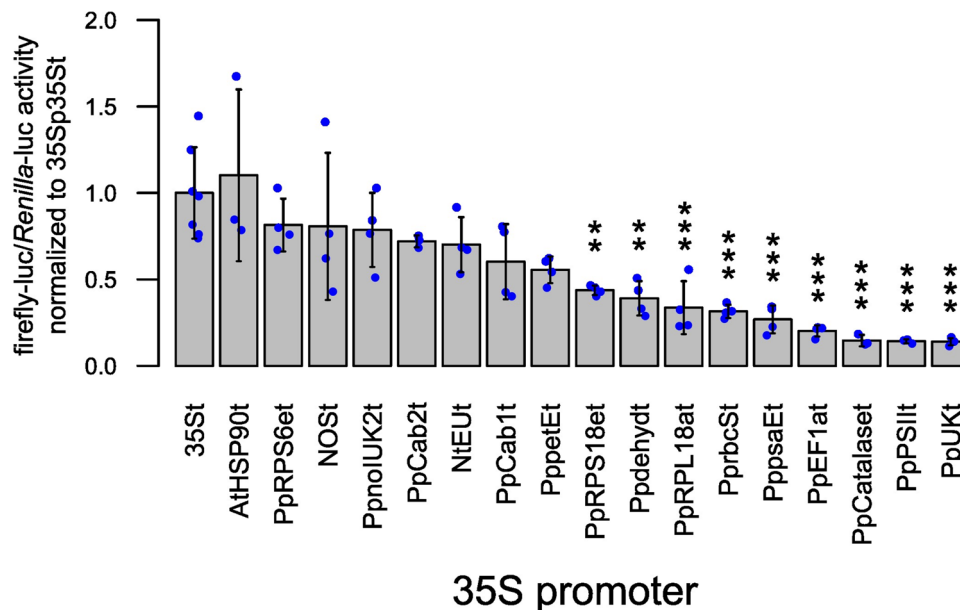


**Fig. 3** Characterization of single terminator candidates. Terminator candidates (Table 1) were cloned into a vector carrying the firefly luciferase coding sequence and the 35S promoter. Terminators were characterized via Dual-Luciferase assay and obtained firefly-luc/*Renilla*-luc reporter values of single candidates normalized to the 35S terminator. Blue dots represent means of three technical rep-

licates of a biological replicate. For each terminator  $n \geq 3$  biological replicates were analysed. Bars represent means of all biological replicates with standard deviations. Significance levels are based on a one-way ANOVA ( $p = 7.91E-11$ ,  $\alpha = 0.05$ ) with subsequent Tukey HSD post hoc test. Indicated differences are between 35St and the respective terminator (\* $p < 0.05$ ; \*\* $p < 0.005$ ; \*\*\* $p < 0.0005$ )

Diamos and Mason 2018). These synergistic effects were observed between terminator pairs depending on their identity, positioning (1st or 2nd), and heterology (heterologous pairs outperformed homologous pairs). This raised the question if different combinations of double terminators would outperform the respective single terminators in *Physcomitrella*. To address this, we generated different combinations of double terminators and tested them using the same experimental setup employed to test the single terminators. First, we generated homologous and heterologous combinations of the two benchmark terminators 35St and NOST. Likewise, we generated combinations of the endogenous terminators PpCab2t and PppetEt. Finally, we generated combinations of a heterologous and an endogenous terminator, AtHSP90t and PpRPS6et. The combinations of 35St and NOST did not show any improvement compared to the respective single terminators, independent of how they were combined (Fig. 4A). In contrast, Diamos and Mason (2018) observed an 18.4-fold increase in GFP reporter signal levels between 35St–NOST double terminator and NOST alone in *N. benthamiana*. Beyene et al. (2011) observed an up to 65-fold increase in EYFP levels between 35St–NOST and 35St in

sugarcane (*Saccharum officinarum*). In contrast, all PpCab2t and PppetEt double terminator combinations outperformed the single terminator petEt in *Physcomitrella* (Fig. 4B). The combination PpCab2t–PppetEt even outperformed both single terminators, yielding around 2.3-fold and 2.9-fold higher than PpCab2t and PppetEt, respectively. PpCab2t–PppetEt also performed higher than the homologous double terminators and even the reciprocal combination PppetEt–PpCab2t. These observations are in line with the findings of Diamos and Mason (2018) regarding the role of identity and positioning of tandem terminators, although the fold changes observed here with an enzymatic reporter were again lower than the fold changes observed in terminator combinations in *N. benthamiana* with a fluorescent reporter.

Moreover, terminator combinations based on AtHSP90t and PpRPS6et depict another deviation from findings in other plant systems. Here, combinations either did not have any deviating effect on performance compared to the respective single terminators, or it decreased performance significantly (Fig. 4C). All terminator combinations containing AtHSP90t yield lower than the respective single terminator, indicating negative interactions between AtHSP90t

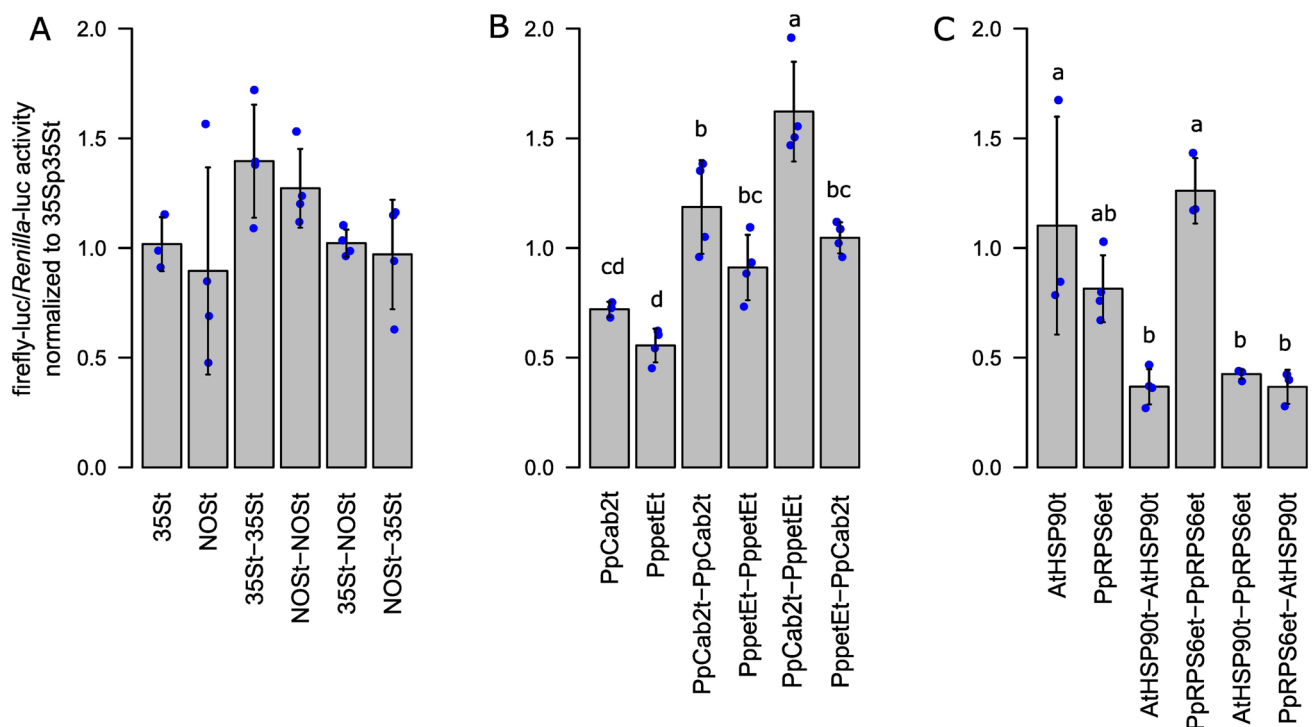


**Fig. 4** Characterization of double terminators. Single terminators were fused in homologous and heterologous pairs in vectors bearing the firefly luciferase coding sequence and the 35S promoter. Double terminators and their respective single terminators were characterized via Dual-Luciferase assays and obtained firefly-luc/*Renilla*-luc reporter values normalized to the 35S terminator. Blue dots represent means of three technical replicates of a biological replicate. Bars represent means of all biological replicates ( $n \geq 3$ )

with standard deviations. No significant difference in performance were observed for combinations of the 35St and NOST (A one-way ANOVA,  $p=0.11$ ,  $\alpha=0.05$ ). Significant differences in performance were observed in combinations of PpCab2t and PppetEt (B one-way ANOVA,  $p=4.16E-7$ ,  $\alpha=0.05$ ) and in combinations of AtHSP90t and PpRPS6et (C one-way ANOVA,  $p=8.42E-05$ ,  $\alpha=0.05$ ). Significance levels and compact letter display are based on a one-way ANOVA with subsequent Tukey HSD post hoc test

and PpRPS6et or itself in *Physcomitrella*. Such a negative effect of AtHSP90t in double terminators was not observed by Yamamoto et al. (2018) when testing AtHSP90t in combination with NtEUt and 35St in *N. benthamiana*.

Taken together, double terminators can have a positive effect on gene expression in *Physcomitrella*. These effects depend strongly on the identity and positioning of the pairs. However, no clear pattern can be deduced at the moment. Also, the performance of certain double terminator combinations, e.g. 35St-NOSSt, seems to vary from species to species.

### Promoters are more dominant in increasing gene expression levels than terminators

In *Physcomitrella*, several promoters were characterized (Horstmann et al. 2004; Jost et al. 2005; Weise et al. 2006; Gitzinger et al. 2009) and PpActin5p, 35Sp and NOSp are among the most employed promoters (Top et al. 2019; Bohlender et al. 2020; Ruiz-Molina et al. 2022a). Data generated in *Arabidopsis* indicate that a terminator's performance is dependent on the promoter it is paired with, suggesting that performance depends more on combinatorial than on additive effects (Andreou et al. 2021). Consequently, the performance of terminators would not be constitutive and must be regarded in relation to the promoter employed. In

this respect, we further analysed the performance of selected terminators in combination with the PpActin5 and the NOS promoter, respectively. Again, reporter values were obtained by normalizing to 35Sp35St which was set to the value 1.

Across the three promoters, no striking difference in terminator performance depending upon the selected promoter was observed (Fig. 3, 5A, B). However, our data reveal the dominant role of the promoter in determining gene expression levels in *Physcomitrella*. As already seen for the 35S promoter (Fig. 3), all tested terminators, except PpnoIUK2t paired with NOSp, performed as well as the 35S terminator (Fig. 5A, B). For the NOS promoter, the terminators 35St, Cab2t, dehydrt, and AtHSP90t perform significantly better than noIUK2t. In the case of the PpActin5 promoter, no significantly different performing pair could be identified. This can be explained by the generally large standard deviation across all terminators combined with the PpActin5 promoter (Fig. 5B). This standard deviation is lower for the 35S promoter (Fig. 3) and even lower for the NOS promoter (Fig. 5A). However, terminators NOSSt and AtHSP90t exhibit an enlarged variation across all three promoters. Our data do not indicate synergistic promoter–terminator interactions to be a prevalent phenomenon in *Physcomitrella*.

Instead, our data clearly show a dominant role of the promoter compared to the terminator when aiming at optimizing gene expression levels. The fold change from lowest to

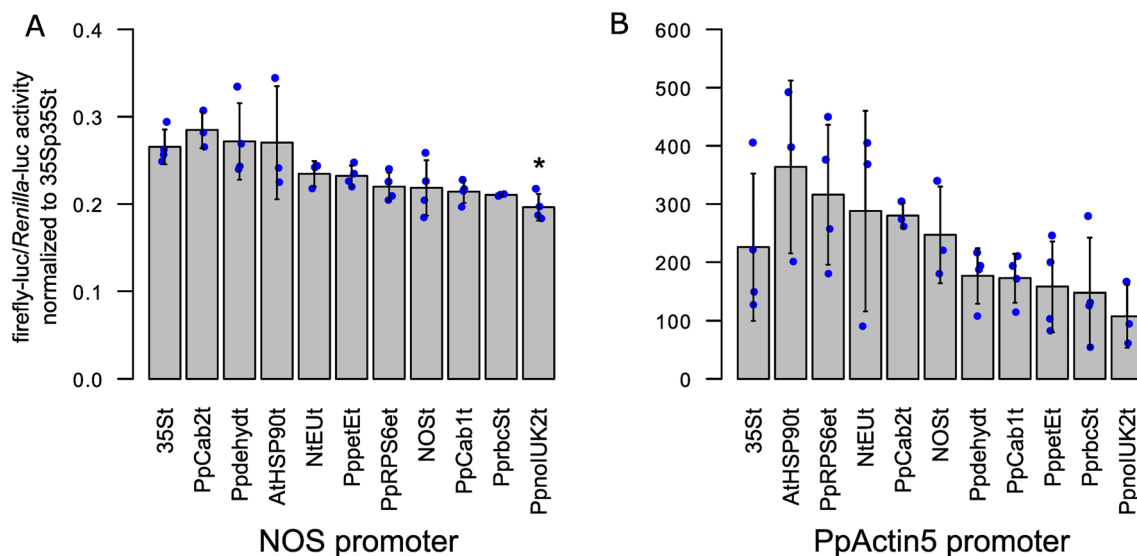


**Fig. 5** Characterization of terminators in combination with the NOS or the PpActin5 promoter. A selection of single terminators was cloned in vectors bearing the firefly luciferase coding sequence and either the **A** NOS promoter or the **B** PpActin5 promoter. The promoter–terminator combinations were characterized via Dual-Luciferase assays and obtained firefly-luc/*Renilla*-luc reporter values normalized to a testing vector bearing the 35S promoter and 35S terminator. Blue dots represent means of three technical replicates of a biological replicate. Bars represent means of all biological replicates

( $n \geq 3$ ) with standard deviations. In combination with the NOS promoter, only terminator PpnoIUK2t shows significant difference in comparison to 35St (**A**, one-way ANOVA,  $p=0.0012$ ,  $\alpha=0.05$ ). For the PpActin5 promoter, no tested terminator significantly differed in performance from 35St (**B**, one-way ANOVA,  $p=0.046$ ,  $\alpha=0.05$ ). Significance levels are based on a one-way ANOVA with subsequent Tukey HSD post hoc test. Indicated differences are between 35St and the respective terminator (\* $p < 0.05$ )

highest performing terminator when using the 35S promoter is 7.9 when comparing 18 different terminator candidates (Fig. 3). For the NOS and PpActin5 promoters, the fold changes are 1.5 and 3.4, respectively, when comparing 11 different terminator candidates (Fig. 5A, B). In turn, AtHSP90t yields 0.27 if combined with the NOS promoter, 1.1 with the 35S promoter, and 363.63 with the PpActin5 promoter, an increase of about 1350-fold. These results clearly underline the importance of choice of promoter over terminator when optimizing gene expression levels. Further, it confirms the superiority of the PpActin5 promoter as compared to the 35S or NOS promoter for recombinant protein production in *Physcomitrella* (Weise et al. 2006).

### Performance is determined by poly(A) signals and sites

Finally, we investigated which of our terminator selection criteria influenced terminator reporter levels the most. For that purpose, Pearson correlation coefficients were calculated between reporter values and different terminator attributes (Table 2). These attributes represent criteria that were applied during terminator selection, e.g., the number of 5'-AATAAA-3' PAS motifs, expression levels from the PEATmoss database (Fernandez-Pozo et al. 2020), and 3'UTR length. In addition, the number of poly(A) sites as predicted via the PASS2.0 software (Ji et al. 2007, 2015) was included, even though this criterion was not applied during terminator candidate selection. Expression values originate from the *Physcomitrella* Gransden wild-type line as seen in Table 1. Since no expression values are available for the non-*Physcomitrella*-derived terminators 35St, NOST, AtHSP90t, and NtEUt; these heterologous terminators were excluded from correlation calculations between reporter levels and expression values.

We found a correlation of  $r=0.71$  between the number of PAS and terminator performance regarding the 35S promoter. In turn, there is only a weak correlation between

PAS and reporter values obtained via the PpActin5 promoter ( $r=0.27$ ) and a weak negative correlation for the NOS promoter ( $r=-0.20$ ). The number of PAS was used as a terminator selection criterion only during the GO term-based approach through which candidates RP-L18a, RP-S6e, and RP-S18e were identified. The presence of PAS did not influence the selection of any other terminator candidates. Still, all non-*Physcomitrella*-derived terminators as well as noI-UK2t and Cab2t exhibit the 5'-AATAAA-3' motif nonetheless (Table 1). Regarding the number of poly(A) sites, terminators characterized via the 35S and PpActin5 promoter show a moderate correlation of  $r=0.5$  and  $r=0.51$ , whereas for the NOS promoter only a weak correlation of  $r=0.27$  was observed. For expression levels, no or only weak correlation was found across reporter values obtained with either of the three promoters. This finding is remarkable, since expression levels were a major criterion in terminator candidate selection. Terminator candidate length exhibits a weak correlation in the PpActin5 and NOS promoter datasets, but no correlation if terminators were combined with the 35S promoter.

Since no or only moderate correlation between the selected single features was observed, we performed principal component analysis (PCA, Fig. 6) to investigate whether combinatorial effects on gene expression can be observed. Expression levels were excluded from this analysis for two reasons: First, the initial Pearson correlation showed no correlation between expression levels and reporter values for either the 35S, NOS, or Actin5 promoter (Table 2). Second, expression levels were obtained from the PEATmoss database (Perroud et al. 2018; Fernandez-Pozo et al. 2020) and are only available for the transcripts of *Physcomitrella* endogenous terminators but not for 35St, NOST, AtHSP90t, and NtEUt. Consequently, these terminators would be excluded from the analysis, thereby minimizing the dataset and thus the validity of the outcome. For the PCA, reporter values for each promoter series were normalized to the promoter series own combination with the 35S terminator, e.g., all reporter values obtained for terminators in combination with the Actin5 promoter were normalized to the sample Act5p35St (Supplementary table S7) to avoid overrating of the strong promoter effects.

The biplot depicts the single data points of promoter–terminator combinations and how these scores are distributed over components (PC) 1 and 2 (Fig. 6A). In addition, the different terminator attributes reporter levels, the number of PAS, the number of poly(A) sites, and length are represented as loading vectors. The length of a vector represents how strongly it impacts the underlying PC, whereas the angle between vectors provides information about the degree of correlation, e.g., a small angle signifies correlation, whereas an angle of 90° signifies a lack of correlation. Using the PCA scores obtained for each promoter–terminator combination,

**Table 2** Pearson correlation coefficients between reporter values and terminator attributes

	# PAS 5'-AATAAA-3'	# Poly(A) sites	Expression levels	Length (bp)
35Sp	0.71	0.50	0.11	0.05
Act5p	0.27	0.51	-0.17	0.33
NOSp	-0.20	0.27	0.04	0.35

Pearson correlation coefficients were calculated between the reporter values obtained and the terminator attributes, such as the number of PAS, number of poly(A) sites, expression levels, and terminator length. The analysis was performed for reporter values obtained with each promoter. For the terminators AtHSP90t, 35St, NtEUt, and NOST expression values were not available

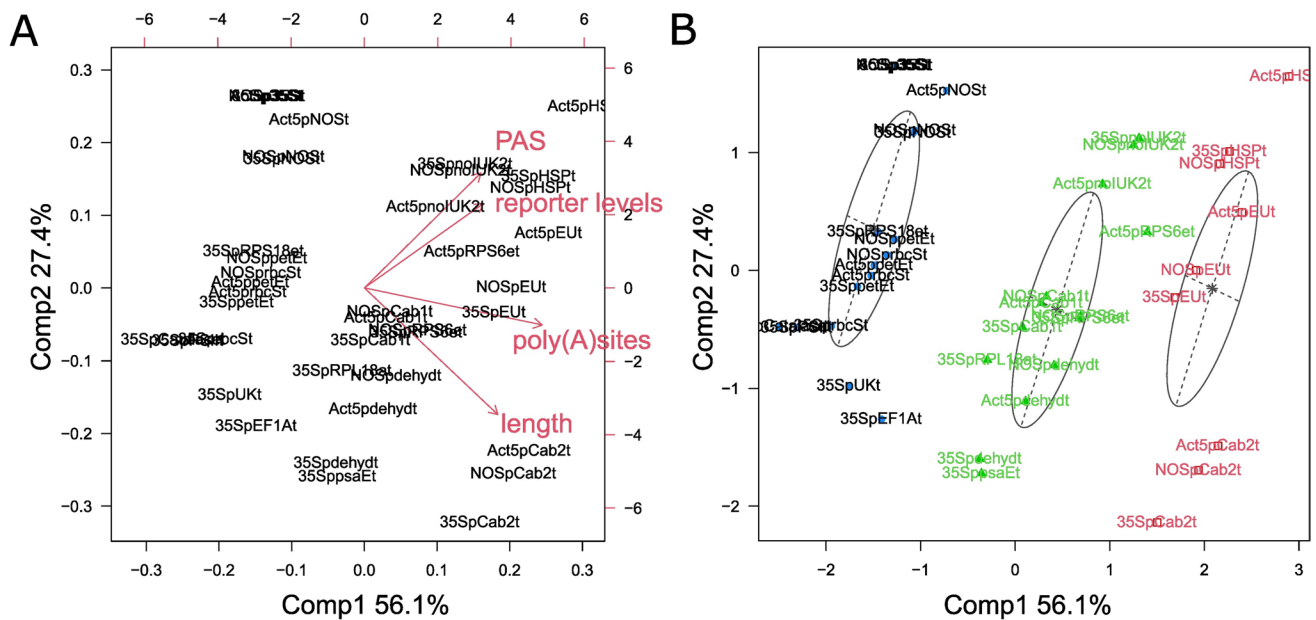


**Fig. 6** Principal component analysis of reporter levels and terminator attributes. A PCA was calculated for the reporter levels obtained, the number of PAS, the number of poly(A) sites, and terminator lengths. Reporter levels of the single promoter series (PpActin5p, 35Sp, NOSP) were normalized to the respective promoter combined with the 35S terminator to remove promoter effects from the dataset. The biplot in **A** shows the different loading vectors of reporter lev-

els and terminator attributes. The PCA plot in **B** shows the result of the model-based clustering using Mclust (Fraley and Raftery 2003). Reporter levels correlate with the number of PAS whereas the number of poly(A) sites and terminator length determine cluster formation. Promoter–terminator combinations are sorted into three clusters in black, green, and red. The scores for each datapoint can be found in Supplementary table S8

we performed model-based clustering using Mclust (Fraley and Raftery 2003). Cluster uncertainties for each datapoint are available in Supplementary table S7.

The biplot in Fig. 6A shows that PC 1 and 2 explain 56.1% and 27.4% of variation, respectively, totalling 83.5%. The number of poly(A) sites has the strongest impact on PC 1, whereas the attributes reporter levels, number of PAS, and length are influencing PC 1 and PC 2 at varying levels. According to this PCA, the length of the terminator and the number of poly(A) sites have the strongest impact on the variance of the data but do not correlate with the obtained reporter values (Fig. 6A). In contrast, the number of PAS correlates with the obtained reporter values.

The PCA plot in Fig. 6B yields three clusters (Supplementary Table S7). The clusters are orientated alongside the loading vectors reporter levels and number of PAS and orthogonal to the loading vectors length and number of poly(A) sites. Accordingly, length and number of poly(A) sites are the main attributes by which clusters were formed. In the red cluster, terminators possess 8–9 poly(A) sites and are on average 518 bp long. Terminators in the green cluster possess 5–7 poly(A) sites and have an average length of 458 bp. In the black cluster, there are terminators with 1–3 poly(A) sites and 304 bp in length. In conclusion, none of the attributes alone is a strong determinant for terminator performance in *Physcomitrella*. Instead, different factors

act to varying degrees on obtained reporter values. Mainly, the number of PAS but also to some degree the number of poly(A) sites influences terminator performance, whereas the terminator length shows a minor effect.

## Discussion

Over decades, the field of molecular pharming and plant biotechnology in general relied on a small range of terminators, namely 35St, NOST, and AtHSP90t. Here, we analysed and selected 3'UTRs of the production host *Physcomitrella* and characterized putative terminator candidates. We further selected high performing candidates for double terminators and tested different combinations and positioning for their effects on gene expression. To address the hypothesis of promoter–terminator interactions we combined a range of terminators with different promoters.

The 3'UTRs of the moss *Physcomitrella* are on average 654 bp long with most sequences at around 400 bp in length. In comparison, 3'UTRs have an average length of 242 bp in *Arabidopsis* and 469 bp in rice (Srivastava et al. 2018). The 3'UTRs of the alga *C. reinhardtii*, in turn, have an average length of 595 bp (Shen et al. 2008a), considerably longer than in *Arabidopsis* and rice and more in line with our findings from *Physcomitrella*. Further, we found

more than 48,000 *Physcomitrella* 3'UTRs to exhibit one or more poly(A) sites, whereas only in 3607 3'UTRs no poly(A) site could be identified. While this finding is in line with data from other plants demonstrating the prevalence of APA in plants, *Physcomitrella* might be more prone to APA than other plants. In *Arabidopsis*, more than 70% of genes contain > 1 poly(A) site according to sequencing the junction of 3'UTRs and poly(A) tails (Wu et al. 2011). In rice, about 50% of genes have > 1 poly(A) sites and 13% have  $\geq 4$  poly(A) sites (Shen et al. 2008b). In *C. reinhardtii*, the number of genes influenced by APA decreases even further to about 33% (Shen et al. 2008a).

We used five determinants to select *Physcomitrella* endogenous terminator candidates from a list of 3'UTRs transcripts (Fig. 2). A main function of terminators is to stabilize mRNAs by facilitating proper polyadenylation which prevents degradation through 3' exonucleases and activation of the mRNA decay pathway. In *N. benthamiana*, long 3'UTRs and 3'UTR-located introns activate NMD of mRNAs (Kertész et al. 2006). In *Arabidopsis*, NMD can act as a viral restriction mechanism by targeting long 3'UTR variants of polycistronic ORFs of potato virus X (Garcia et al. 2014). These findings are in line with data obtained in yeast (*S. cerevisiae*) showing least active terminators to be linked to longer 3'UTRs. In contrast, a genome-wide analysis of *Arabidopsis* NMD rates and their determinants showed 3'UTRs longer than 300 bp and the presence of introns in the 3'UTRs to not influence mRNA half-lives (Narsai et al. 2007). In *Physcomitrella*, not 3'UTR length but splicing within the 3'UTR, especially if close to the stop codon, is a positive predictor of NMD (Lloyd et al. 2018). As a result, we chose a relatively high 3'UTR cut-off value of 400 bp due to the ambiguous findings regarding the effect of 3'UTR length on mRNA as well as the higher average length of *Physcomitrella* 3'UTRs compared to other plants. Even though not actively selected against, the cut-off at 400 bp removed all but one intron-containing terminator candidate from the list (UK2t) (Table 1). Still, for characterization of UK2 the intron-less version (noIUK2t) was used, based on the findings of Lloyd et al. (2018), showing that splicing in the 3'UTR correlates with NMD in *Physcomitrella*. In addition, the intron-less NtEUt yielded higher reporter levels compared to the intron-containing version in *N. benthamiana* (Rosenthal et al. 2018). Further, an over-representation (CAGTTGAAATTT and GTGAAAVTTTTTC) and under-representation (CCAACATCAT, CTTGGCTA, and THTCA WGGGT) of certain motifs in NMD-targeted transcripts was found (Lloyd et al. 2018). In *Arabidopsis*, destabilizing motifs were generally rich in T, whereas stabilizing motifs were rich in A, including the conserved PAS motif 5'-AAT AAA-3' (Loke et al. 2005; Narsai et al. 2007) used for terminator selection in this study. For both *Physcomitrella* and *Arabidopsis*, the authors state that in many cases, transcripts

contained motifs of both kinds, suggesting a yet unclear interplay of motifs and their effect on transcript stability. Further, the sequence identity of the most prevalent PAS in *Physcomitrella* has not been identified and could vary substantially from the *Arabidopsis* PAS as is the case for *C. reinhardtii* (PAS: TG TAA) (Wodniok et al. 2007). Moreover, studies across yeast, humans, and plants demonstrated mRNA half-lives to be linked to the biological process of the encoded protein (Wang et al. 2002; Yang et al. 2003; Narsai et al. 2007; Yamanishi et al. 2013). mRNAs encoding for proteins involved in central metabolism, energy, protein synthesis, and subcellular localization showed significantly higher half-lives in *Arabidopsis* as compared to transcripts classified in highly regulated processes, such as stress response-related transcription factors and kinases (Narsai et al. 2007). Accordingly, many of the 11 *Physcomitrella* terminator candidates not selected via GO term enrichment analysis are also linked to central metabolism and photosynthesis (Table 1). miRNAs negatively impact mRNA half-lives due to their established role in complementary RNA targeting, cleavage, and degradation (Jones-Rhoades et al. 2006; Narsai et al. 2007) and were therefore used as a determinant for terminator candidate selection.

As NtEUt, NOST, and AtHSP90t are among the highest yielding terminators in *Physcomitrella*, this demonstrates the versatility of some gene expression elements across plant lineages (moss, angiosperm). Across three different angiosperms (*N. benthamiana*, *N. tabacum*, lettuce), a slightly varying but nevertheless strong effect of NtEUt on reporter expression levels could be demonstrated (Diamos & Mason 2018). Further, the functionality of NtEUt and NtEUt-based double terminators in a range of angiosperm species and tissues, such as lettuce (*Lactuca sativa*), eggplant (*Solanum melongena*), tomato (*Solanum lycopersicum*) fruits and leaves, hot peppers (*Capsicum frutescens*), melons (*Cucumis melo*), orchids (*Phalaenopsis Aphrodite*), and roses (*Rosa* sp. 'Bonheur'), could be shown (Yamamoto et al. 2018). However, reporter levels were not quantified in that study. Here, we demonstrated EUt from *N. tabacum* to be functional in *Physcomitrella*. However, an increase in gene expression for NtEUt as compared to 35St and NOST in *N. benthamiana* (Diamos and Mason 2018; Rosenthal et al. 2018) could not be obtained in *Physcomitrella*. This may hint at differences between mosses and angiosperms in the use of terminators for the regulation of gene expression.

A selection of terminators was further characterized using the promoters NOSp and PpActin5p (Fig. 5). Here, we found relatively small fold changes from lowest to highest performing terminator of 1.5 and 3.4 for NOSp and PpActin5p, respectively. As for the 35S promoter, heterologous terminators NtEUt, AtHSP90t, and NOST, as well as five *Physcomitrella* endogenous terminators performed as well as the default terminator 35St. However, large fold changes

in reporter levels between the promoters NOSp, 35Sp, and PpActin5p were obvious. We further found the effect of the promoter to be independent of the paired terminator. In *Arabidopsis*, synergistic effects between promoters and terminators were reported by characterizing 15 terminators in combination with five different promoters (Andreou et al. 2021). They found AtHSP90t to perform consistently high, AtrbcS2b to perform consistently low, and NOST to perform in dependence of the paired promoter. Here, we tested at least 11 terminators across three promoters and could not identify clear promoter–terminator interactions in *Physcomitrella*. Indeed, terminators, such as NOST and noIUK2t, show varying performance across promoters in this moss. Further, AtHSP90t and PprbcSt also performed consistently high or low, respectively, across promoters. This finding is similar to data described by Andreou et al. (2021) for AtHSP90t and AtrbcS2b. Overall, the data obtained here indicate that in *Physcomitrella*, the choice of terminator does not have a huge impact on gene expression levels. Instead, the selection of the promoter has a larger impact and dominates the influence in gene expression in our assay.

After characterizing the selected terminator candidates via the Dual-Luciferase system, we aimed to clarify how the selection criteria influenced terminator performance the most (Table 2). A PCA for which expression levels were excluded revealed that the number of PAS and the number of poly(A) sites influence terminator performance in *Physcomitrella* (Fig. 6). This is not surprising, since both attributes are involved in the main function of terminators, namely terminating transcription and facilitating pre-mRNA processing into mature mRNAs through polyadenylation of the transcript's 3' end (Bentley 2005; Mandel et al. 2008). Proper polyadenylation further influences mRNA export from the nucleus, transcript stability, and translation rates (Hoshino 2012; Paek et al. 2015; Choe et al. 2018). However, PAS and poly(A) sites do not govern terminator performance alone. In *Arabidopsis*, stepwise deletion of PAS motifs from the AtHSP90t terminator did not reduce terminator performance (Andreou et al. 2021). In turn, 32 nucleotides at the 5' end of AtHSP90t had a significant effect on reporter levels in *N. benthamiana*, even though this sequence does not contain any known motifs acting in polyadenylation (de Felippes et al. 2022). Combining the AtHSP90t 5' with other terminators, similar to creating double terminators, further increased reporter levels. Respective transcripts did not differ in number or distribution of poly(A) sites or length of the poly(A) tail. Instead, a reduction in transcriptional read through and generation of small RNAs acting in transcript decay was observed.

In *N. benthamiana*, two terminators were identified and found to exceed reporter levels of the 35S terminator when tested in that same plant system (Diamos and Mason 2018). These elements were identified by searching for stabilizing

motifs in 3'UTRs to identify terminator candidates, based on Narsai et al. (2007), who identified stabilizing and destabilizing motifs in *Arabidopsis* 3'UTRs (Diamos and Mason 2018). Interestingly, the list of stabilizing motifs includes the canonical PAS 5'-AATAAA-3' as well as its reverse sequence 5'-AAATAA-3', indicating RNA-binding *trans*-elements to be direction unspecific. Looking at other selection criteria used here, our results indicate that expression values did not have a large impact on terminator performance in *Physcomitrella*. At the same time, our results show the huge effect promoters have on gene expression as compared to terminators. Therefore, transcript abundance, which is the ratio of transcription rate to turnover rate, might be influenced to a larger extent by the promoter and therefore does not constitute an ideal criterion for terminator candidate selection. Likewise, the PCA demonstrated that terminator length did not exhibit a conclusive effect on terminator performance (Fig. 6). On the one hand, this observation fits with the findings by Lloyd et al. (2018), who showed that long 3'UTRs in *Physcomitrella* are not a positive predictor of NMD. On the other hand, we only characterized terminators in the range of 211 bp (35St) to 611 bp (Cab2t), which is still below the average length of 3'UTRs in *Physcomitrella* of 654 bp (Fig. 1). Consequently, our observation does not apply to *Physcomitrella* 3'UTRs in general but only to the length range tested here. In conclusion, of the selection criteria applied here for terminator candidate selection, the number of PAS and the number of poly(A) sites impact terminator performance notably, whereas terminator length and transcript abundance have a minor impact (Fig. 6, Table 2). In addition, other factors such as the presence or absence of stabilizing or destabilizing motifs can act as good predictors for future terminator selection.

Subsequently, we analysed if combinations of two terminators would increase reporter gene levels. In *Physcomitrella*, the highest increases in signal strength by double terminators were achieved by the pairs Cab2t-petEt (ca. 1.6-fold). Of all the double terminators tested here, including pairs based on 35St and NOST, as well as RPS6et and AtHSP90t, the pair Cab2t-petEt is the only combination which yielded more than the respective single terminators. As in *N. benthamiana* (Diamos and Mason 2018), we also observed that the effect of double terminators on gene expression depended on relative positioning. This indicates that this effect is based on interactions between the respective terminators as opposed to additive effects. Whether heterologous or homologous pairs are preferable cannot be concluded here.

The decrease in reporter signal levels for all combinations containing AtHSP90t is surprising. So far, AtHSP90t was combined with NtEUt, NOST, NbHSpt, 35St, and itself, but for none of these pairs, a negative effect of AtHSP90t was observed in *N. benthamiana* (Diamos and Mason 2018;

Yamamoto et al. 2018). Also, the pairs consisting of 35St & NOST behave differently here as compared to other systems. Beyene et al. (2011) showed an increase in EYFP signal strength in transient particle bombardment assays in *N. tabacum* of up to 65-fold for 35St-NOST in comparison to 35St alone. Diamos and Mason (2018) evaluated relative GFP and dsRed production via analysis of fluorescence levels visualized on UV-illuminated SDS-PAGE gels in *N. benthamiana* and found a change of > fivefold for 35St-NOST compared to 35St, whereas other combinations reached > 25-fold increases in reporter levels. One explanation for these discrepancies might be species-specific effects. However, 35St and NOST are used as single terminators in a range of different plant species, including *Physcomitrella*. Since double terminators are generally functional in *Physcomitrella* and this effect is believed to be based on terminator–terminator interactions, it is surprising that 35St & NOST double terminator pairs in *Physcomitrella* do not perform as well as in angiosperms. It is argued that double terminators lead to more stringent transcription termination and polyadenylation and less aberrant RNA, thereby reducing RDR6-mediated post translational gene silencing (PTGS) (Diamos and Mason 2018). This argumentation is in line with findings in *Arabidopsis* where truncated and non-polyadenylated transcripts did not accumulate in wild-type plants but increased to higher levels in *rdr6* mutants (Luo and Chen 2007). Further, usage of double terminators decreased mRNA 3' read through and specific siRNA accumulation while increasing gene expression. It is argued that while RDR6-mediated PTGS might play a substantial role in explaining the positive effect of double terminators, it does not explain synergistic effects between terminators (Andreou et al. 2021). Instead, it is hypothesized that the positive effect of double terminators is also connected to promoter–terminator interactions. These interactions occur during gene looping when 5' and 3'UTRs associate through bound members of the transcription machinery. A second terminator with additional and/or differing binding motifs for members of the polyadenylation complex could therefore interact more strongly with transcription factors bound to the 5' end, resulting in more efficient gene looping and gene expression (Andreou et al. 2021). In *Drosophila*, a connection was found between the transcriptional start site (TSS) of a gene and the choice of poly(A) site, resulting in preferred TSS–poly(A) site pairs, which differed depending on the analysed tissue (Alfonso-Gonzalez et al. 2023). However, in *Physcomitrella*, we observed the effect of double terminators on gene expression but found no indication for synergistic promoter–terminator effects.

Taken together, our data do not allow the deduction of any rules to predict how double terminators influence gene expression in *Physcomitrella* based on positioning and identity of the pair. However, observed effects do not behave

additively but instead show positive and negative synergies. The mechanisms behind the effect of double terminators remains elusive. In general, double terminators can be an effective measure to increase molecular pharming yields which is why the mechanism behind double terminators should be elucidated further. For that purpose, methods to quantify transcriptional read through and PTGS and identify preferred poly(A) sites can be employed (Rosenthal et al. 2018; de Felippes et al. 2020; Shah et al. 2021). To investigate differences in transcriptional regulation between mosses and angiosperms, terminators with shown discrepancies between the two systems are of interest, such as 35St and NOST pairs as well as AtHSP90t-based double terminators.

Besides species-specific effects, different reporter systems may be a reason for discrepancies in characterization data of genetic elements. Most publications reporting large changes between different terminators and double terminators used a reporter system based on fluorescence proteins such as GFP and RFP (Beyene et al. 2011; Diamos and Mason 2018; Rosenthal et al. 2018). While these results are promising for the utility of 3'UTRs and especially double terminators in boosting molecular pharming yields, other publications demonstrate a considerably smaller but nevertheless significant effect of terminators (Yamamoto et al. 2018; Tian et al. 2022; Chamness et al. 2023), in line with our findings in *Physcomitrella*. Yamamoto (2018) reported changes below twofold in *N. benthamiana* for double terminators based on different combinations of AtHSP90t, NtEUt, and 35St using gel densitometry of Coomassie-stained SDS-PAGE gels. Using the Dual-Luciferase reporter system in *N. benthamiana*, less than twofold difference between NOST compared to NtEUt or 35St-NbACT7t-Rb7 was found (Chamness et al. 2023). The combination of 35St and NbACT7t with the matrix attachment region Rb7 was initially reported to yield a > 60-fold increase in reporter levels compared to NOST using a fluorophore-based reporter system (Diamos and Mason 2018). In line with our findings, a maximum of 2.6-fold difference among 13 terminators characterized in both agroinfiltrated *N. benthamiana* leaves and BY2 cell culture was shown via the Dual-Luciferase system (Tian et al. 2022). Further, the authors compared promoter characterization data obtained via Dual-Luciferase assays to GFP reporter assays by verifying the data using RT qPCR. For the Dual-Luciferase system, they found a correlation of 0.89 between firefly transcript and measured reporter values, whereas for GFP reporter assays a correlation of only 0.64 was found (Tian et al. 2022). Consequently, this indicates potential flaws in using fluorescence reporters for characterization of gene expression elements. A possible explanation might be the degree of autofluorescence emitted by plant cells and fluorescence signal interference with chlorophyll. In contrast, the Dual-Luciferase system is based on chemiluminescence using unique substrates for both firefly and



*Renilla* luciferases and is generally considered more sensitive than fluorescence-based assays (Naylor 1999). However, the relatively short half-lives of firefly luciferase (2–3 h) (Thompson et al. 1991; Ignowski and Schaffer 2004) as compared to GFP (26 h) (Corish and Tyler-Smith 1999) might also explain the difference in the results obtained. Rosenthal et al. (2018) evaluated NtEUt using a GFP reporter, the GUS reporter system, and by quantifying Norwalk virus capsid protein via ELISA. The authors observed a 2.8-fold increase for NtEUt as compared to 35St using the GFP reporter. This difference decreased to around twofold using the GUS reporter system and less than 1.5-fold when using ELISA, thereby nicely demonstrating discrepancies between the different reporter systems used in characterizing elements of gene expression.

Besides different reporter systems, the use of transient assays versus stably transformed lines may influence the outcome. Here, we characterized terminators via transient protoplast transformation, whereas molecular pharming in *Physcomitrella* is performed in stably transformed lines. Generally, double terminators and other elements of gene expression such as matrix attachment regions (MARs) are functional also in transgenic lines (Luo and Chen 2007; Ji et al. 2013). However, only a few studies are available which directly compare the two methods using the same plant species and reporter system. No differences were found when comparing repressible synthetic promoter systems in stably and transiently transformed *Arabidopsis* protoplasts using the Dual-Luciferase system (Schaumberg et al. 2016). Likewise, also in *Arabidopsis*, the AtHSP90 terminator yielded 2.5-fold higher GUS reporter values than NOST, irrespective of the transformation method (Nagaya et al. 2010). In contrast, the MAR TM6 increased GUS reporter levels higher than MAR Rb7 in transgenic tobacco, whereas in transiently transformed cells using a GFP reporter system, Rb7 performed higher than TM6 (Ji et al. 2013; Damos and Mason 2018). To conclude, characterization data for elements of gene expression can differ widely depending on the employed reporter system and whether tested in transiently or stably transformed cells. This constitutes a problem regarding the comparability of published data, a concern that adds to the already existing complexity caused by species-specific effects.

In conclusion, we have described *Physcomitrella* 3'UTRs at the whole genome level, and identified and characterized 14 new endogenous terminator sequences. As a result, we obtained a selection of terminator sequences performing as well as established terminators 35St, AtHSP90t, and NOST. Subsequent analysis of our terminator candidate selection criteria revealed polyadenylation-related motifs to be positive predictors of terminator performance. Double terminators also have the potential to increase gene expression levels in *Physcomitrella*, although no clear patterns in how double

terminator composition affects outcome could be ascertained. Observed performance differences between single and double terminators in *Physcomitrella* and angiosperms may hint at evolutionary changes in the impact of terminators on gene expression.

**Supplementary Information** The online version contains supplementary material available at <https://doi.org/10.1007/s00299-023-03088-5>.

**Acknowledgements** The authors appreciate language editing by Anne Katrin Prowse.

**Author contributions** PAN designed research, performed experiments, analysed data, and wrote the manuscript. PE analysed data. SW performed experiments. JP and ELD designed research. SNWH designed research, analysed data, and helped writing the manuscript. RR designed and supervised research, acquired funding, and wrote the manuscript. All authors read and approved the final version of the manuscript.

**Funding** Open Access funding enabled and organized by Projekt DEAL. This work was supported by Marie Skłodowska-Curie Actions Innovative Training Network under the Horizon 2020 programme under Grant Agreement No. 765115 (MossTech) and by the German Research Foundation (DFG) under Germany's Excellence Strategy (CIBSS-EXC-2189-Project ID 390939984). P.A.N. gratefully acknowledges financial support by Studienstiftung des deutschen Volkes.

**Data availability** All terminator sequences identified in this study are deposited on GenBank (GenBank identifier: Terminator—OR204709: Cab1t, OR204710: dehyd1, OR204711: petEt, OR204712: Cab2t, OR204713: Catalaset, OR204714: PSII, OR204715: UKt, OR204716: rbcSt, OR204717: EF1At, OR204718: psaEt, OR204719: RP-L18At, OR204720: RP-S6et, OR204721: RP-S18et, OR204722: UK2t).

## Declarations

**Conflict of interest** Authors declare no competing interests.

**Open Access** This article is licensed under a Creative Commons Attribution 4.0 International License, which permits use, sharing, adaptation, distribution and reproduction in any medium or format, as long as you give appropriate credit to the original author(s) and the source, provide a link to the Creative Commons licence, and indicate if changes were made. The images or other third party material in this article are included in the article's Creative Commons licence, unless indicated otherwise in a credit line to the material. If material is not included in the article's Creative Commons licence and your intended use is not permitted by statutory regulation or exceeds the permitted use, you will need to obtain permission directly from the copyright holder. To view a copy of this licence, visit <http://creativecommons.org/licenses/by/4.0/>.

## References

- Alfonso-Gonzalez C, Legnini I, Holec S, Arrigoni L, Ozbulut HC, Mateos F, Koppstein D, Rybak-Wolf A, Bönisch U, Rajewsky N, Hilgers V (2023) Sites of transcription initiation drive mRNA isoform selection. *Cell* 186:2438–2455. <https://doi.org/10.1016/j.cell.2023.04.012>
- Andreou AI, Nirkko J, Ochoa-Villarreal M, Nakayama N (2021) Mobius assembly for plant systems highlights promoter-terminator

- interaction in gene regulation. bioRxiv. <https://doi.org/10.1101/2021.03.31.437819>
- Bentley DL (2005) Rules of engagement: co-transcriptional recruitment of pre-mRNA processing factors. *Curr Opin Cell Biol* 17:251–256. <https://doi.org/10.1016/j.ceb.2005.04.006>
- Beyene G, Buenrostro-Nava MT, Damaj MB, Gao S-J, Molina J, Mirkov TE (2011) Unprecedented enhancement of transient gene expression from minimal cassettes using a double terminator. *Plant Cell Rep* 30:13–25. <https://doi.org/10.1007/s00299-010-0936-3>
- Bohlender LL, Parsons J, Hoernstein SNW, Rempfer C, Ruiz-Molina N, Lorenz T, Rodríguez Jahnke F, Figl R, Fode B, Altmann F, Reski R, Decker EL (2020) Stable protein sialylation in *Physcomitrella*. *Front Plant Sci* 11:610032. <https://doi.org/10.3389/FPLS.2020.610032>
- Büttner-Mainik A, Parsons J, Jérôme H, Hartmann A, Lamer S, Schaaf A, Schlosser A, Zipfel PF, Reski R, Decker EL (2011) Production of biologically active recombinant human factor H in *Physcomitrella*. *Plant Biotechnol J* 9:373–383. <https://doi.org/10.1111/J.1467-7652.2010.00552.X>
- Capell T, Twyman RM, Armario-Najera V, Ma JKC, Schillberg S, Christou P (2020) Potential applications of plant biotechnology against SARS-CoV-2. *Trends Plant Sci* 25:635–643. <https://doi.org/10.1016/j.tplants.2020.04.009>
- Chamness JC, Kumar J, Cruz AJ, Rhuby E, Holum MJ, Cody JP, Tibebu R, Gamo ME, Starker CG, Zhang F, Voytas DF (2023) An extensible vector toolkit and parts library for advanced engineering of plant genomes. *Plant Genome* 16:e20312. <https://doi.org/10.1002/tpg2.20312>
- Choe J, Lin S, Zhang W, Liu Q, Wang L, Ramirez-Moya J, Du P, Kim W, Tang S, Sliz P, Santisteban P, George RE, Richards WG, Wong KK, Locker N, Slack FJ, Gregory RI (2018) mRNA circularization by METTL3–eIF3h enhances translation and promotes oncogenesis. *Nature* 561:556–560. <https://doi.org/10.1038/s41586-018-0538-8>
- Chui M, Evers M, Manyika J, Zheng A, Nisbet T (2020) The bio revolution innovations transforming economies, societies, and our lives. [www.mckinsey.com/mgi](http://www.mckinsey.com/mgi)
- Corish P, Tyler-Smith C (1999) Attenuation of green fluorescent protein half-life in mammalian cells. *Protein Eng* 12:1035–1040. <https://doi.org/10.1093/PROTEIN/12.12.1035>
- D'Aoust MA, Couture MMJ, Charland N, Trépanier S, Landry N, Ors F, Vézina LP (2010) The production of hemagglutinin-based virus-like particles in plants: a rapid, efficient and safe response to pandemic influenza. *Plant Biotechnol J* 8:607–619. <https://doi.org/10.1111/J.1467-7652.2009.00496.X>
- Dai X, Zhao PX (2011) psRNATarget: a plant small RNA target analysis server. *Nucleic Acids Res* 39:W155–159. <https://doi.org/10.1093/nar/gkr319>
- Dai X, Zhuang Z, Zhao PX (2018) psRNATarget: a plant small RNA target analysis server (2017 release). *Nucleic Acids Res* 46:W49–W54. <https://doi.org/10.1093/NAR/GKY316>
- de Felippes FF, McHale M, Doran RL, Roden S, Eamens AL, Finnegan EJ, Waterhouse PM (2020) The key role of terminators on the expression and post-transcriptional gene silencing of transgenes. *Plant J* 104:96–112. <https://doi.org/10.1111/tpj.14907>
- de Felippes FF, Shand K, Waterhouse PM (2022) Identification of a transferrable terminator element that inhibits small RNA production and improves transgene expression levels. *Front Plant Sci* 13:877793. <https://doi.org/10.3389/fpls.2022.877793>
- Decker EL, Reski R (2020) Mosses in biotechnology. *Curr Opin Biotechnol* 61:21–27. <https://doi.org/10.1016/j.copbio.2019.09.021>
- Decker EL, Wiedemann G, Reski R (2015) Gene targeting for precision glyco-engineering: production of biopharmaceuticals devoid of plant-typical glycosylation in moss bioreactors. *Methods Mol Biol* 1321:213–224. [https://doi.org/10.1007/978-1-4939-2760-9\\_15](https://doi.org/10.1007/978-1-4939-2760-9_15)
- Diamos AG, Mason HS (2018) Chimeric 3' flanking regions strongly enhance gene expression in plants. *Plant Biotechnol J* 16:1971–1982. <https://doi.org/10.1111/pbi.12931>
- Egener T, Granado J, Guitton M-C, Hohe A, Holtorf H, Lucht JM, Rensing SA, Schlink K, Schulte J, Schween G, Zimmermann S, Duwenig E, Rak B, Reski R (2002) High frequency of phenotypic deviations in *Physcomitrella patens* plants transformed with a gene-disruption library. *BMC Plant Biol* 2:6. <https://doi.org/10.1186/1471-2229-2-6>
- Fernandez-Pozo N, Haas FB, Meyberg R, Ullrich KK, Hiss M, Perroud P-F, Hanke S, Kratz V, Powell AF, Vesty EF, Daum CG, Zane M, Lipzen A, Sreedasyam A, Grimwood J, Coates JC, Barry K, Schmutz J, Mueller LA, Rensing SA (2020) PEATmoss (*Physcomitrella* Expression Atlas Tool): a unified gene expression atlas for the model plant *Physcomitrella patens*. *Plant J* 102:165–177. <https://doi.org/10.1111/tpj.14607>
- Fraley C, Raftery A (2003) Enhanced model-based clustering, density estimation, and discriminant analysis software: MCLUST. *J Classif* 20:263–286. <https://doi.org/10.1007/s00357-003-0015-3>
- Garcia D, Garcia S, Voinnet O (2014) Nonsense-mediated decay serves as a general viral restriction mechanism in plants. *Cell Host Microbe* 16:391–402. <https://doi.org/10.1016/J.CHOM.2014.08.001>
- Gitzinger M, Parsons J, Reski R, Fussenegger M (2009) Functional cross-kingdom conservation of mammalian and moss (*Physcomitrella patens*) transcription, translation and secretion machineries. *Plant Biotechnol J* 7:73–86. <https://doi.org/10.1111/J.1467-7652.2008.00376.X>
- Goodstein DM, Shu S, Howson R, Neupane R, Hayes RD, Fazo J, Mitros T, Dirks W, Hellsten U, Putnam N, Rokhsar DS (2012) Phytozome: a comparative platform for green plant genomics. *Nucleic Acids Res* 40:D1178–D1186. <https://doi.org/10.1093/NAR/GKR944>
- Guo C, Spinelli M, Liu M, Li QQ, Liang C (2016) A genome-wide study of “non-3UTR” polyadenylation sites in *Arabidopsis thaliana*. *Sci Rep* 6:28060. <https://doi.org/10.1038/SREP28060>
- He W, Baysal C, Lobato Gómez M, Huang X, Alvarez D, Zhu C, Armario-Najera V, Blanco Perera A, Cerda Bennaser P, Saba-Mayoral A, Sobrino-Mengual G, Vargheese A, Abranches R, Alexandra Abreu I, Balamurugan S, Bock R, Buyel JF, da Cunha NB, Daniell H, Capell T (2021) Contributions of the international plant science community to the fight against infectious diseases in humans—part 2: affordable drugs in edible plants for endemic and re-emerging diseases. *Plant Biotechnol J* 19:1921–1936. <https://doi.org/10.1111/PBI.13658>
- Hennermann JB, Arash-Kaps L, Fekete G, Schaaf A, Busch A, Frischmuth T (2019) Pharmacokinetics, pharmacodynamics, and safety of moss- $\alpha$ Galactosidase A in patients with Fabry disease. *J Inherit Metab Dis* 42:527–533. <https://doi.org/10.1002/JIMD.12052>
- Hoernstein SNW, Fode B, Wiedemann G, Lang D, Niederkrueger H, Berg B, Schaaf A, Frischmuth T, Schlosser A, Decker EL, Reski R (2018) Host cell proteome of *Physcomitrella patens* harbors proteases and protease inhibitors under bioproduction conditions. *J Proteome Res* 17:3749–3760. <https://doi.org/10.1021/acs.jproteome.8b00423>
- Hohe A, Reski R (2002) Optimisation of a bioreactor culture of the moss *Physcomitrella patens* for mass production of protoplasts. *Plant Sci* 163:69–74. [https://doi.org/10.1016/S0168-9452\(02\)00059-6](https://doi.org/10.1016/S0168-9452(02)00059-6)
- Hohe A, Egener T, Lucht JM, Holtorf H, Reinhard C, Schween G, Reski R (2004) An improved and highly standardised transformation procedure allows efficient production of single and multiple

- targeted gene-knockouts in a moss, *Physcomitrella patens*. *Curr Genet* 44:339–347. <https://doi.org/10.1007/S00294-003-0458-4>
- Horstmann V, Huether CM, Jost W, Reski R, Decker EL (2004) Quantitative promoter analysis in *Physcomitrella patens*: a set of plant vectors activating gene expression within three orders of magnitude. *BMC Biotechnol* 4:13. <https://doi.org/10.1186/1472-6750-4-13>
- Hoshino S (2012) Mechanism of the initiation of mRNA decay: role of eRF3 family G proteins. *Wires RNA* 3:743–757. <https://doi.org/10.1002/wrna.1133>
- Hunt AG (2008) Nuclear pre-mRNA processing in plants—messenger RNA 3' end formation in plants. Springer Berlin Heidelberg, pp 151–177. [https://doi.org/10.1007/978-3-540-76776-3\\_9](https://doi.org/10.1007/978-3-540-76776-3_9)
- Ignowski JM, Schaffer DV (2004) Kinetic analysis and modeling of firefly luciferase as a quantitative reporter gene in live mammalian cells. *Biotechnol Bioeng* 86:827–834. <https://doi.org/10.1002/BIT.20059>
- Ji G, Zheng J, Shen Y, Wu X, Jiang R, Lin Y, Loke JC, Davis KM, Reese GJ, Li QQ (2007) Predictive modeling of plant messenger RNA polyadenylation sites. *BMC Bioinformatics* 8:43. <https://doi.org/10.1186/1471-2105-8-43>
- Ji L, Xu R, Lu L, Zhang J, Yang G, Huang J, Wu C, Zheng C (2013) TM6, a novel nuclear matrix attachment region enhances its flanking gene expression through influencing their chromatin structure. *Mol Cells* 36:127–137. <https://doi.org/10.1007/10059-013-0092-z>
- Ji G, Li L, Li QQ, Wu X, Fu J, Chen G, Wu X (2015) PASPA: a web server for mRNA poly(A) site predictions in plants and algae. *Bioinformatics* 31:1671–1673. <https://doi.org/10.1093/bioinformatics/btv004>
- Jones-Rhoades MW, Bartel DP, Bartel B (2006) MicroRNAs and their regulatory roles in plants. *Annu Rev Plant Biol* 57:19–53. <https://doi.org/10.1146/ANNUREV.ARPLANT.57.032905.105218>
- Jost W, Link S, Horstmann V, Decker EL, Reski R, Gorr G (2005) Isolation and characterisation of three moss-derived beta-tubulin promoters suitable for recombinant expression. *Curr Genet* 47:111–120. <https://doi.org/10.1007/S00294-004-0555-Z>
- Kertész S, Kerényi Z, Mérai Z, Bartos I, Pálffy T, Barta E, Silhavy D (2006) Both introns and long 3'-UTRs operate as cis-acting elements to trigger nonsense-mediated decay in plants. *Nucleic Acids Res* 34:6147–6157. <https://doi.org/10.1093/nar/gkl737>
- Khraiwesh B, Arif M, Seumel G, Ossowski S, Weigel D, Reski R, Frank W (2010) Transcriptional control of gene expression by microRNAs. *Cell* 140:111–122. <https://doi.org/10.1016/j.cell.2009.12.023>
- Koprivova A, Stemmer C, Altmann F, Hoffmann A, Kopriva S, Gorr G, Reski R, Decker EL (2004) Targeted knockouts of *Physcomitrella* lacking plant-specific immunogenic N-glycans. *Plant Biotechnol J* 2:517–523. <https://doi.org/10.1111/J.1467-7652.2004.00100.X>
- Lang D, Ullrich KK, Murat F, Fuchs J, Jenkins J, Haas FB, Piednoel M, Gundlach H, Van Bel M, Meyberg R, Vives C, Morata J, Symeonidi A, Hiss M, Muchero W, Kamisugi Y, Saleh O, Blanc G, Decker EL, van Gessel N, Grimwood J, Hayes RD, Graham SW, Gunter LE, McDaniel S, Hoernstein SNW, Larsson A, Li F-W, Phillips J, Ranjan P, Rokhsar DS, Rothfels CJ, Schneider L, Shu S, Stevenson DW, Thümmel F, Tillich M, Villarreal A, JC, Widiez T, Wong GK-S, Wymore A, Zhang Y, Zimmer AD, Quatrano RS, Mayer KFX, Goodstein D, Casacuberta JM, Vandepoele K, Reski R, Cuming AC, Tuskan J, Maumus F, Salse J, Schmutz J, Rensing SA (2018) The *Physcomitrella patens* chromosome-scale assembly reveals moss genome structure and evolution. *Plant J* 93:515–533. <https://doi.org/10.1111/TPJ.13801>
- Li XQ, Du D (2014) Motif types, motif locations and base composition patterns around the RNA polyadenylation site in microorganisms, plants and animals. *BMC Evol Biol* 14:162. <https://doi.org/10.1186/S12862-014-0162-7>
- Li Q, Hunt AG (1997) The polyadenylation of RNA in plants. *Plant Physiol* 115:321–325. <https://doi.org/10.1104/pp.115.2.321>
- Liu W, Brooks EG, Elorriaga E, Liu Y, Dudit JR, Yuan G, Tsai CJ, Tuskan GA, Ranney TG, Yang X (2023) Plant promoters and terminators for high-precision bioengineering. *BioDesign Res*. <https://doi.org/10.34133/bdr.0013>
- Lloyd JPB, Lang D, Zimmer AD, Causier B, Reski R, Davies B (2018) The loss of SMG1 causes defects in quality control pathways in *Physcomitrella patens*. *Nucleic Acids Res* 46:5822–5836. <https://doi.org/10.1093/NAR/GKY225>
- Lobato Gómez M, Huang X, Alvarez D, He W, Baysal C, Zhu C, Armario-Najera V, Blanco Perera A, Cerda Bennasser P, Saba-Mayoral A, Sobrino-Mengual G, Vargheese A, Abranches R, Abreu IA, Balamurugan S, Bock R, Buyel JF, da Cunha NB, Daniell H, Christou P (2021) Contributions of the international plant science community to the fight against infectious diseases in humans - part 1: epidemic and pandemic diseases, including HIV/AIDS and coronaviruses. *Plant Biotechnol J* 19:1901–1920. <https://doi.org/10.1111/PBI.13657>
- Loke JC, Stahlberg EA, Strenski DG, Haas BJ, Wood PC, Li QQ (2005) Compilation of mRNA polyadenylation signals in Arabidopsis revealed a new signal element and potential secondary structures. *Plant Physiol* 138:1457–1468. <https://doi.org/10.1104/pp.105.060541>
- Lomonosoff GP, D'Aoust M-A (2016) Plant-produced biopharmaceuticals: a case of technical developments driving clinical deployment. *Science* 353:1237–1240. <https://doi.org/10.1126/science.aaf6638>
- Luo Z, Chen Z (2007) Improperly terminated, unpolysadenylated mRNA of sense transgenes is targeted by RDR6-mediated RNA silencing in Arabidopsis. *Plant Cell* 19:943–958. <https://doi.org/10.1105/tpc.106.045724>
- Macfarlane SA, Gilmer D, Davies JW (1992) Efficient inoculation with CaMV 35 S promoter-driven DNA clones of the tobamovirus PEBV. *Virology* 187:829–831. [https://doi.org/10.1016/0042-6822\(92\)90488-B](https://doi.org/10.1016/0042-6822(92)90488-B)
- Mandel CR, Bai Y, Tong L (2008) Protein factors in pre-mRNA 3'-end processing. *Cell Mol Life Sci* 65:1099–1122. <https://doi.org/10.1007/s00018-007-7474-3>
- Margolin E, Chapman R, Williamson AL, Rybicki EP, Meyers AE (2018) Production of complex viral glycoproteins in plants as vaccine immunogens. *Plant Biotechnol J* 16:1531–1545. <https://doi.org/10.1111/pbi.12963>
- Mayr C (2016) Evolution and biological roles of alternative 3'UTRs. *Trends Cell Biol* 26:227–237. <https://doi.org/10.1016/J.TCB.2015.10.012>
- Medina R, Johnson MG, Liu Y, Wickett NJ, Shaw AJ, Goffinet B (2019) Phylogenomic delineation of *Physcomitrium* (Bryophyta: Funariaceae) based on targeted sequencing of nuclear exons and their flanking regions rejects the retention of *Physcomitrella*, *Physcomitridium* and *Aphanorrhagma*. *J Syst Evol* 57:404–417. <https://doi.org/10.1111/JSE.12516>
- Michelfelder S, Parsons J, Bohlender LL, Hoernstein SNW, Niederkrüger H, Busch A, Krieghoff N, Koch J, Fode B, Schaaf A, Frischmuth T, Pohl M, Zipfel PF, Reski R, Decker EL, Häffner K (2017) Moss-produced, glycosylation-optimized human Factor H for therapeutic application in complement disorders. *J Am Soc Nephrol* 28:1462–1474. <https://doi.org/10.1681/ASN.2015070745>
- Michelfelder S, Fischer F, Wäldin A, Hörle KV, Pohl M, Parsons J, Reski R, Decker EL, Zipfel PF, Skerka C, Häffner K (2018) The MFHR1 fusion protein is a novel synthetic multitarget complement inhibitor with therapeutic potential. *J Am Soc Nephrol* 29:1141–1153. <https://doi.org/10.1681/ASN.2017070738>

- Moore MJ, Proudfoot NJ (2009) Pre-mRNA processing reaches back to transcription and ahead to translation. *Cell* 136:688–700. <https://doi.org/10.1016/j.cell.2009.02.001>
- Nagaya S, Kawamura K, Shinmyo A, Kato K (2010) The HSP terminator of *Arabidopsis thaliana* increases gene expression in plant cells. *Plant Cell Physiol* 51:328–332. <https://doi.org/10.1093/pcp/pcp188>
- Narsai R, Howell KA, Millar AH, O'Toole N, Small I, Whelan J (2007) Genome-wide analysis of mRNA decay rates and their determinants in *Arabidopsis thaliana*. *Plant Cell* 19:3418–3436. <https://doi.org/10.1105/TPC.107.055046>
- Naylor LH (1999) Reporter gene technology: the future looks bright. *Biochem Pharmacol* 58:749–757. [https://doi.org/10.1016/S0006-2952\(99\)00096-9](https://doi.org/10.1016/S0006-2952(99)00096-9)
- Paek KY, Hong KY, Ryu I, Park SM, Keum SJ, Kwon OS, Jang SK (2015) Translation initiation mediated by RNA looping. *Proc Natl Acad Sci USA* 112:1041–1046. <https://doi.org/10.1073/PNAS.1416883112>
- Parsons J, Altmann F, Arrenberg CK, Koprivova A, Beike AK, Stemmer C, Gorr G, Reski R, Decker EL (2012) Moss-based production of asialo-erythropoietin devoid of Lewis A and other plant-typical carbohydrate determinants. *Plant Biotechnol J* 10:851–861. <https://doi.org/10.1111/J.1467-7652.2012.00704.X>
- Perroud P-F, Haas FB, Hiss M, Ullrich KK, Alboresi A, Amirebrahimi M, Barry K, Bassi R, Bonhomme S, Chen H, Coates JC, Fujita T, Guyon-Debast A, Lang D, Lin J, Lipzen A, Nogué F, Oliver MJ, Ponce de León I, Rensing SA (2018) The *Physcomitrella patens* gene atlas project: large-scale RNA-seq based expression data. *Plant J* 95:168–182. <https://doi.org/10.1111/tpj.13940>
- Pietrzak M, Shillito RD, Hohn T, Potrykus I (1986) Expression in plants of two bacterial antibiotic resistance genes after protoplast transformation with a new plant expression vector. *Nucleic Acids Res* 14:5857. <https://doi.org/10.1093/NAR/14.14.5857>
- Reski R (2018) Quantitative moss cell biology. *Curr Opin Plant Biol* 46:39–47. <https://doi.org/10.1016/J.PBI.2018.07.005>
- Reski R, Abel WO (1985) Induction of budding on chloronemata and caulonemata of the moss, *Physcomitrella patens*, using isopentenyladenine. *Planta* 165:354–358. <https://doi.org/10.1007/BF00392232>
- Reski R, Parsons J, Decker EL (2015) Moss-made pharmaceuticals: from bench to bedside. *Plant Biotech J* 13:1191–1198. <https://doi.org/10.1111/pbi.12401>
- Reski R, Bae H, Simonsen HT (2018) *Physcomitrella patens*, a versatile synthetic biology chassis. *Plant Cell Rep* 37:1409–1417. <https://doi.org/10.1007/s00299-018-2293-6>
- Rosenthal SH, Damos AG, Mason HS (2018) An intronless form of the tobacco extensin gene terminator strongly enhances transient gene expression in plant leaves. *Plant Mol Biol* 96:429–443. <https://doi.org/10.1007/s11103-018-0708-y>
- Rothnie HM (1996) Plant mRNA 3'-end formation. *Plant Mol Biol* 32:43–61. <https://doi.org/10.1007/BF00039376>
- Rothnie HM, Chen G, Fütterer J, Hohn T (2001) Polyadenylation in rice tungro bacilliform virus: cis-acting signals and regulation. *J Virol* 75:4184–4194. <https://doi.org/10.1128/JVI.75.9.4184-4194.2001>
- Ruiz-Molina N, Parsons J, Müller M, Hoernstein SNW, Bohlender LL, Pumple S, Zipfel PF, Häffner K, Reski R, Decker EL (2022a) A synthetic protein as efficient multitarget regulator against complement over-activation. *Commun Biol* 5:152. <https://doi.org/10.1038/s42003-022-03094-5>
- Ruiz-Molina N, Parsons J, Schroeder S, Posten C, Reski R, Decker EL (2022b) Process engineering of biopharmaceutical production in moss bioreactors via model-based description and evaluation of phytohormone impact. *Front Bioeng Biotechnol* 10:837965. <https://doi.org/10.3389/FBIOE.2022.837965>
- Rybicki EP (2020) Plant molecular farming of virus-like nanoparticles as vaccines and reagents. *Wires Nanomed Nanobiotechnol* 12:e1587. <https://doi.org/10.1002/wnan.1587>
- Schaaf A, Tintelnot S, Baur A, Reski R, Gorr G, Decker EL (2005) Use of endogenous signal sequences for transient production and efficient secretion by moss (*Physcomitrella patens*) cells. *BMC Biotechnol* 5:30. <https://doi.org/10.1186/1472-6750-5-30>
- Schaumberg KA, Antunes MS, Kassaw TK, Xu W, Zalewski CS, Medford JI, Prasad A (2016) Quantitative characterization of genetic parts and circuits for plant synthetic biology. *Nat Methods* 13:94–100. <https://doi.org/10.1038/nmeth.3659>
- Schween G, Hohe A, Koprivova A, Reski R (2003) Effects of nutrients, cell density and culture techniques on protoplast regeneration and early protonema development in a moss, *Physcomitrella patens*. *J Plant Physiol* 160:209–212. <https://doi.org/10.1078/0176-1617-00855>
- Shah A, Mittleman BE, Gilad Y, Li YI (2021) Benchmarking sequencing methods and tools that facilitate the study of alternative polyadenylation. *Genome Biol* 22:291. <https://doi.org/10.1186/s13059-021-02502-z>
- Shen Y, Liu Y, Liu L, Liang C, Li QQ (2008a) Unique features of nuclear mRNA Poly(A) signals and alternative polyadenylation in *Chlamydomonas reinhardtii*. *Genetics* 179:167–176. <https://doi.org/10.1534/GENETICS.108.088971>
- Shen Y, Ji G, Haas BJ, Wu X, Zheng J, Reese GJ, Li QQ (2008b) Genome level analysis of rice mRNA 3'-end processing signals and alternative polyadenylation. *Nucleic Acids Res* 36:3150–3161. <https://doi.org/10.1093/NAR/GKN158>
- Shen JS, Busch A, Day TS, Meng XL, Yu CI, Dabrowska-Schlepp P, Fode B, Niederkrüger H, Forni S, Chen S, Schiffmann R, Frischmuth T, Schaaf A (2016) Mannose receptor-mediated delivery of moss-made  $\alpha$ -galactosidase A efficiently corrects enzyme deficiency in Fabry mice. *J Inher Metab Dis* 39:293–303. <https://doi.org/10.1007/S10545-015-9886-9>
- Srivastava AK, Lu Y, Zinta G, Lang Z, Zhu JK (2018) UTR-dependent control of gene expression in plants. *Trends Plant Sci* 23:248–259. <https://doi.org/10.1016/J.TPLANTS.2017.11.003>
- Stropp R, Scholz S, Kruse S, Speth V, Reski R (1998) Plant nuclear gene knockout reveals a role in plastid division for the homolog of the bacterial cell division protein FtsZ, an ancestral tubulin. *Proc Natl Acad Sci USA* 95:4368–4373. <https://doi.org/10.1073/PNAS.95.8.4368>
- Tan-Wong SM, Wijayatilake HD, Proudfoot NJ (2009) Gene loops function to maintain transcriptional memory through interaction with the nuclear pore complex. *Genes Dev* 23:2610–2624. <https://doi.org/10.1101/gad.1823209>
- Tan-Wong SM, Zaugg JB, Camblong J, Xu Z, Zhang DW, Mischo HE, Ansari AZ, Luscombe NM, Steinmetz LM, Proudfoot NJ (2012) Gene loops enhance transcriptional directionality. *Science* 338:671–675. <https://doi.org/10.1126/science.1224350>
- Thompson JF, Hayes LS, Lloyd DB (1991) Modulation of firefly luciferase stability and impact on studies of gene regulation. *Gene* 103:171–177. [https://doi.org/10.1016/0378-1119\(91\)90270-L](https://doi.org/10.1016/0378-1119(91)90270-L)
- Tian C, Zhang Y, Li J, Wang Y (2022) Benchmarking intrinsic promoters and terminators for plant synthetic biology research. *BioDesign Res* 2022:9834989. <https://doi.org/10.34133/2022/9834989>
- Top O, Parsons J, Bohlender LL, Michelfelder S, Kopp P, Busch-Steenberg C, Hoernstein SNW, Zipfel PF, Häffner K, Reski R, Decker EL (2019) Recombinant production of MFHR1, a novel synthetic multitarget complement inhibitor, in moss bioreactors. *Front Plant Sci* 10:260. <https://doi.org/10.3389/FPLS.2019.00260>
- Top O, Milferstädt SWL, van Gessel N, Hoernstein SNW, Özdemir B, Decker EL, Reski R (2021) Expression of a human cDNA in moss results in spliced mRNAs and fragmentary

- protein isoforms. *Commun Biol* 4:964. <https://doi.org/10.1038/s42003-021-02486-3>
- Twyman RM, Stoger E, Schillberg S, Christou P, Fischer R (2003) Molecular farming in plants: host systems and expression technology. *Trends Biotechnol* 21:570–578. <https://doi.org/10.1016/j.tibtech.2003.10.002>
- Wang Y, Liu CL, Storey JD, Tibshirani RJ, Herschlag D, Brown PO (2002) Precision and functional specificity in mRNA decay. *Proc Natl Acad Sci USA* 90:5860–5865. <https://doi.org/10.1073/pnas.092538799>
- Ward BJ, Makarkov A, Séguin A, Pillet S, Trépanier S, Dhaliwall J, Libman MD, Vesikari T, Landry N (2020) Efficacy, immunogenicity, and safety of a plant-derived, quadrivalent, virus-like particle influenza vaccine in adults (18–64 years) and older adults (≥ 65 years): two multicentre, randomised phase 3 trials. *Lancet* 396:P1491–1503. [https://doi.org/10.1016/S0140-6736\(20\)32014-6](https://doi.org/10.1016/S0140-6736(20)32014-6)
- Weise A, Rodriguez-Franco M, Timm B, Hermann M, Link S, Jost W, Gorr G (2006) Use of *Physcomitrella patens* actin 5' regions for high transgene expression: importance of 5' introns. *Appl Microbiol Biotechnol* 70:337–345. <https://doi.org/10.1007/s00253-005-0087-6>
- Wodniok S, Simon A, Glöckner G, Becker B (2007) Gain and loss of polyadenylation signals during evolution of green algae. *BMC Evol Biol* 7:65. <https://doi.org/10.1186/1471-2148-7-65>
- Wu X, Liu M, Downie B, Liang C, Ji G, Li QQ, Hunt AG (2011) Genome-wide landscape of polyadenylation in *Arabidopsis* provides evidence for extensive alternative polyadenylation. *Proc Natl Acad Sci* 108:12533. <https://doi.org/10.1073/pnas.1019732108>
- Yamamoto T, Hoshikawa K, Ezura K, Okazawa R, Fujita S, Takao M, Mason HS, Ezura H, Miura K (2018) Improvement of the transient expression system for production of recombinant proteins in plants. *Sci Rep* 8:4755. <https://doi.org/10.1038/s41598-018-23024-y>
- Yamanishi M, Ito Y, Kintaka R, Imamura C, Katahira S, Ikeuchi A, Moriya H, Matsuyama T (2013) A genome-wide activity assessment of terminator regions in *Saccharomyces cerevisiae* provides a “Terminatome” toolbox. *ACS Synth Biol* 2:337–347. <https://doi.org/10.1021/sb300116y>
- Yang E, van Nimwegen E, Zavolan M, Rajewsky N, Schroeder M, Magnasco M, Darnell JE (2003) Decay rates of human mRNAs: correlation with functional characteristics and sequence attributes. *Genome Res* 13:1863. <https://doi.org/10.1101/GR.1272403>
- Zhao H, Xing D, Li QQ (2009) Unique features of plant cleavage and polyadenylation specificity factor revealed by proteomic studies. *Plant Physiol* 151:1546–1556. <https://doi.org/10.1104/pp.109.142729>
- Zhong V, Archibald BN, Brophy JAN (2023) Transcriptional and post-transcriptional controls for tuning gene expression in plants. *Curr Opin Plant Biol* 71:102315. <https://doi.org/10.1016/j.pbi.2022.102315>
- Zimmer AD, Lang D, Buchta K, Rombauts S, Nishiyama T, Hasebe M, Van de Peer Y, Rensing SA, Reski R (2013) Reannotation and extended community resources for the genome of the non-seed plant *Physcomitrella patens* provide insights into the evolution of plant gene structures and functions. *BMC Genomics* 14:498. <https://doi.org/10.1186/1471-2164-14-498>

**Publisher's Note** Springer Nature remains neutral with regard to jurisdictional claims in published maps and institutional affiliations.